Chapter 6
Segmented SRF Cryomodules

E. Daly, Thomas H. Nicol and J. Preble

Abstract Linear accelerators based on Superconducting Radio Frequency (SRF) cavities have become increasingly important and wide spread. This chapter reviews the design and operation of four different SRF segmented cryomodules. These cryomodules were used in projects from the 1980s to the 2010s and as such this chapter provides a good overview of the development of this type of cryostat. Topics described include: requirements, cooling of SRF cavities, tuners, power couplers, structural and thermal insulation systems, magnetic shields, vacuum systems and instrumentation. Performance results from both prototypes and series operation are presented.

6.1 Introduction

An important application of cryogenics in particle accelerators is the cooling of Superconducting Radiofrequency (SRF) cavities. These cavities provide acceleration to the charged particle beam by storing radiofrequency (RF) energy in a resonant structure (or cavity). The system is designed such that the electrical field produced in the SRF cavity accelerates the charged particles as they pass through the cavity. The cavities are made from pure niobium operated in its superconducting state to minimize the wall losses of the RF energy. Thus, more of the input RF energy goes into accelerating the beam itself.

E. Daly (✉) · J. Preble
Thomas Jefferson National Laboratory, 12000 Jefferson Avenue,
Newport News, VA 23606, USA
e-mail: edaly@jlab.org

J. Preble
e-mail: preble@jlab.org

T.H. Nicol
Fermi National Accelerator Laboratory, P.O. Box 500, Batavia
IL 60510, USA
e-mail: tnicol@fnal.gov

J.G. Weisend II (ed.), *Cryostat Design*, International Cryogenics Monograph Series,
DOI 10.1007/978-3-319-31150-0_6

Since this application involves RF energy and is thus an alternating current application of superconductivity, there are always going to be wall losses and heating within the superconducting niobium. These losses are a function of a number of parameters including the RF frequency and the temperature. The optimal temperature for most SRF applications is between 1.8 and 2.1 K.

The SRF cavities are built into cryostats known as cryomodules. These are described below and in Chap. 5. In addition to the cavities themselves, SRF cryomodules contain other components. Power couplers (or couplers) bring the RF energy from the room temperature power supplies to the SRF cavities. Tuners adjust the resonant frequency of the cavities by physically changing the cavities shape. Higher order mode (HOM) couplers remove unwanted frequencies generated by the beam moving through the SRF cavity. A complementary approach is to absorb the HOM frequencies in a dissipative material to prevent its propagation. Such materials are known as HOM absorbers or HOM loads. In addition, the cryomodules typically contain magnetic shielding to protect the cavities from stray magnetic fields (including the earth's) which can degrade cavity performance.

Requirements for cryomodules include: low heat leak, low vibration, tight alignment tolerances on the cavities and a high vacuum level in the beam tube vacuum for optimum cavity performance.

There are two ways that cryogenic and vacuum systems are distributed to individual modules in superconducting magnets or cavity strings. The first, referred to as fine segmentation or segmented, refers to systems in which the insulating vacuum and the cryogenic circuits are confined to an individual cryomodule or cryostat with the only connection between modules being the beam tube. This approach has a number of advantages; it may allow for individual warm up and cool down of cryomodules, the separate cryostat isolation vacuums prevents a failure in one isolation vacuum space from propagating to other cryostats and the space in between the segmented cryomodules may be filled with magnets, beam instrumentation and vacuum systems that are more easily operated at 300 K. Fine segmentation is the most common approach used in SRF cryomodules and is seen in the examples given in this chapter as well as in the European Spallation Source (ESS) [1] and Facility for Rare Isotope Beams (FRIB) [2] projects.

There are disadvantages to fine segmentation. The biggest is that the many warm to cold transitions add additional heat leak and are quite expensive. Thus, for systems involving large numbers of cryostats or cryomodules, the second approach sometimes called coarse segmentation or continuous is used. Course segmentation refers to systems in which the cryogenic circuits and insulating vacuum inside individual cryostats are more or less continuous for long lengths, at least over the length of several cryomodules. Accelerator magnet systems such as the SSC (Chap. 2) and the LHC (Chap. 3) are configured this way as are the SRF cryomodules envisioned for the ILC, LCLS II and the XFEL at DESY (Chap. 5).

Generally speaking, systems involving less than 100 cryostats or cryomodules use the segmented approach while those involving more than 100 components use the continuous approach.

This chapter describes the design and experience of four different segmented cryomodules. The cryomodules are described in rough chronological order of their design and were designed between the 1980s and the 2010s. Since these cryomodules have many similar requirements, their design solutions are similar. However, an evolution of design can be also seen over the course of the development of these cryomodules. Due to the historical nature of these descriptions, the units used as those in place at the time of the original designs. Thus, a mixture of SI and English units will be seen.

6.2 C20 Cryomodule Design for CEBAF

6.2.1 Introduction

The Continuous Electron Beam Accelerator Facility (CEBAF) was built as a 4 GeV, 200 μA, electron accelerating facility [3]. The C20 cryomodule is the original design for the CEBAF accelerator and was developed in the late 1980's. CEBAF was the world's largest installation of Superconducting Radio Frequency (SRF) accelerating cavities. CEBAF had 338 identical SRF cavities housed in 43 cryostats. The cavities were assembled in pairs which became the natural design segment for the cryomodules. Four of these pairs were housed in identical cryostats that would be assembled together along with end cans to form a single cryomodule (see Fig. 6.1). The exception to this was the first cryostat, a quarter cryomodule, which included a single cavity pair cryostat with end caps.

6.2.2 Modularity and Segmentation

The CEBAF accelerator (see Fig. 6.2) includes two antiparallel linacs, an injector, and three experimental halls. Each linac contains 25 repeating zones. The first 20 of these zones contain one C20 cryomodule each. A zone is 10 m long and contains a cryomodule and a warm beamline girder which are 8.35 and 1.65 m long respectively. Each cryomodule has two helium supplies and returns, a primary circuit operating at 2 K and a shield circuit operating at 50 K, eight SRF cavities with 5 kW radio frequency (RF) power feeds, and various electrical connections for RF

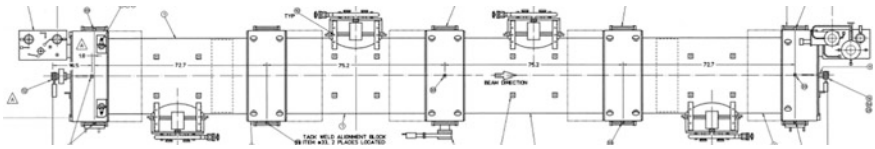

Fig. 6.1 C20 CEBAF cryomodule

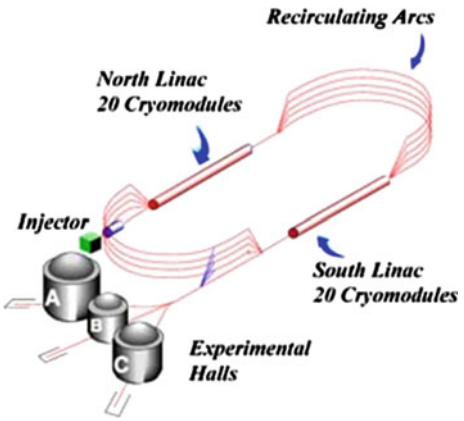

Fig. 6.2 CEBAF accelerator

signals, instrumentation, and motor controls for the helium supply valve and cavity tuner stepper motors. A cryomodule can be removed and replaced with another cryomodule or drift tube in about a week minimizing accelerator operational down time. This has been valuable over the life of the machine as eleven cryomodules have been removed and refurbished over the first 23 years of operation.

6.2.3 Requirements

The cryomodule requirements were detailed in a design handbook that covered the entire CEBAF accelerator ensuring appropriate system integration. The top level cryomodule requirements include an operating voltage of 20 MV, capable of accelerating 200 μA of beam recirculated five times, a nominal operating heat load of 68 and 140 W for the primary and shield circuits respectively. The eight SRF cavities contained in a cryomodule are required to be aligned relative to the nominal beam trajectory with a root-mean-square angular position of 2 mR and centered on the beam axis to ±0.02 in. The detailed requirements contained in the design handbook are the extension of these high level requirements to individual systems or components. Table 6.1 shows a summary of these requirements.

6.2.4 Design Description and Choices

The original CEBAF cryomodule was the first large scale installation of SRF technology in the US. The adoption of this new technology was a risk and many design choices were made to allow for testing and verification of the cavity

Table 6.1 Summary of CEBAF C20 cryomodule requirements from CEBAF design handbook (1991 revision)

Item	Value	Units
Number of cryomodules	42.25	
Number of such sections used in injector	2.25	
Number of such sections used in linac	40	
Length of section, including magnetic elements	9.60	m
Number of cryounits per cryomodule	4	
Number of cavities per cryomodule	8	
Cavities		
Type	Superconducting	
Duty cycle	CW	
Operating frequency	1497, ±0.00002	MHz
Accelerating gradient, active length	≥5	MV/m
Intrinsic limitation of accelerating gradient	≥20	MV/m
Power coupled into beam, per cavity	2.5	kW
Total linac-associated power consumption	≤10	MW
HOM impedances, for most important modes	500, 170,000	
Regenerative beam breakup threshold, per beamlet	>200	Actual μA
Regenerative beam breakup threshold, per beamlet	>2000	Computed μA
Current transport capability	1000	μA
Number of cells per cavity	5	
Operating mode	π	
Cell shape	Elliptical	
Fundamental power coupler, waveguide	Beamline	
HOM coupler	Beamline	
Output waveguide cutoff frequency	1900	MHz
Number of output waveguides	2	
Angle between waveguides	90	
Elastic pressure sensitivity	<60	Hz/torr
Microphonic tolerance, cryomodule surface	10	microns/sec
Cryostat (cryounit)		
Thermal intercept shield	1	
Magnetic shield	2	
Liquid Level probe	1	
Superinsulation blankets	2	
Support rods	10	
Heater (100 W in liquid bath)	1	
Cryogenic thermometers (minimum)	2	
Bridge piece set		
Bridging ring, insulating vacuum	1	
Thermal shield closure with braided hose	1	
Superinsulation blankets	2	
Magnetic shield	1	
Beampipe with pump out	1	
Helium pumping line, with bellows	1	

performance during assembly and to minimize potential for compromising the demonstrated performance by subsequent processes. Two SRF cavities were assembled into a hermetically sealed Cavity Pair (CP), see Fig. 6.3, which undergoes performance testing in a Vertical Test Area (VTA) [4] and are never vented after testing to avoid contamination.

The cavities have frequency tuners installed and this assembly is mounted in a 316L stainless steel helium vessel. The helium vessel is assembled into a cryostat that includes cold and warm layers of magnetic shielding, an intermediate temperature thermal shield, multilayer insulation and a vacuum vessel. Together this assembly is a Cryounit (CU) see Fig. 6.4. Four of these CUs are assembled with a supply and return cryogenic end can to make a Cryomodule (CM). The cryomodule is the smallest assembly that is transported to and installed in the accelerator.

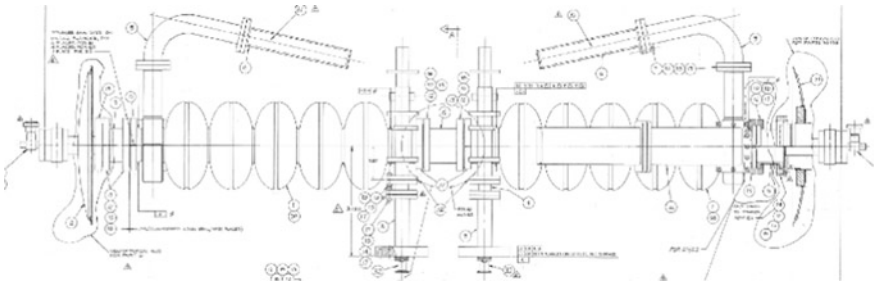

Fig. 6.3 C20 cavity pair

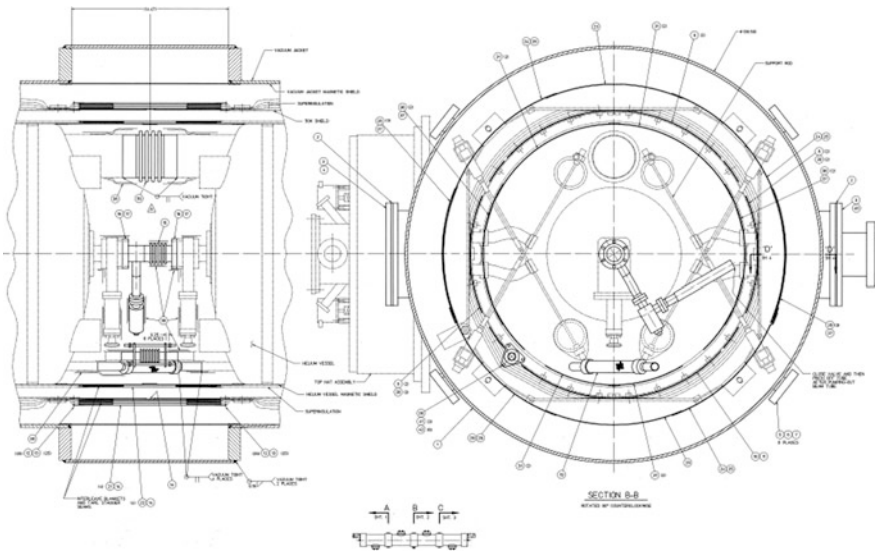

Fig. 6.4 Bridging area between two cryounits

6.2.5 Cryogenic System Interfaces

Helium is supplied from a large central helium cryogenic plant [5] by a vacuum jacketed distribution system [6]. At each cryomodule there are two supply and two return bayonet connections. A cryomodule has two mating bayonet connections in each end can. A typical connection in the cryomodule is a female bayonet with a ball valve for isolation and a safety relief valve. All volumes that can have cold helium trapped inside include safety relief valves. The supply end can includes a primary and shield 3.8 cm bayonets. The primary supply carries 3 bar, 2.2 K helium to a J-T valve. The J-T valve is controlled to maintain a set liquid level in the cryomodule of 2 K, 0.031 bar liquid helium. The shield supply line is a 3 atm 40 K helium line with no valves internal to the cryomodule. The return end can includes two bayonets and a primary circuit relief stack. The primary supply bayonet is a larger 7.9 cm bayonet to support pumping the required mass flow at the lower return pressure. The shield return bayonet is the same size as the supply. The relief stack is designed for high flow rates due to the large liquid inventory and potential for very high heat loads in the event of a loss of vacuum in the cryostat. There is a two stage relief setting. A lower pressure, 1.2 atm, relief is sized for the maximum mass flow through the inlet J-T valve and a higher pressure, 4.1 atm differential, relief valve is sized for the flow associated with a loss of vacuum [7]. Both relief valves are reseating designs. All cryogenic connection between air and sub-atmospheric helium include a double o-ring seal with vacuum pumping between the o-rings to ensure air is not allowed to leak into the cryogenic circuit.

6.2.6 Vacuum Interfaces

The CEBAF linacs are separated from the warm beam transport vacuum chambers as they include cold components that will cryopump all gasses and accumulate contamination over time. The separation of the vacuum spaces is done with a differential vacuum pump, an electrostatic precipitator, and a fast gate valve. The combination of these elements is designed to protect against off normal vacuum events in the warm beam transport chambers. The cryomodule has three separate vacuum systems, the beamline which include one 30 L per second ion pump, insulating vacuum, and the RF power coupler which includes one 20 L per second ion pump each. The cryomodule beamline interface to the warm girder is an electro-pneumatic controlled 70 mm viton sealed gate valve. The insulating vacuum has a single manually actuated 152 mm viton sealed gate valve that is connected to a pumping station for initial pump down and maintenance as needed. The RF power couplers are configured with a manifold allowing two couplers to be pumped by a single ion pump. The manifold has a 70 mm manual right angle viton o-ring sealed valve used initial pump down and maintenance operations.

6.2.7 Heat Load Estimates

The CEBAF cryomodule is dominated by dynamic RF heat loads. The cavity specification allows for a maximum dynamic heat load of 5.4 W per cavity. Due to improved gradient performance of the cavities over the specification the typical operating conditions for the cavities are at $\sim$150 % of the design values [8]. Along with a dynamic waveguide heat load this accounts for the $\sim$100 W of dynamic 2 K heat load. The static heat load budget for each cryomodule is 18 W and has been measured to be closer to 14 W on average. The static heat load has several components including the bayonets, beamline transitions from 2 to 300 K, and the RF power couplers. The shield static heat load is measured at $\sim$150 W and comes from the heat stationing of the bayonets, beamlines transitions and the RF power couplers.

6.2.8 Cavity

The LE5 SRF cavity developed at Cornell's University's Newman Laboratory, has five cells resonant at 1497 MHz, one fundamental power coupler (FPC) located at one end of the cavity and two higher order mode couplers (HOM) located at the opposite end. The FPC and HOM are waveguide couplers sized for specific RF cutoff frequencies. The cavity is fabricated from high RRR sheet metal niobium. The cavity is operated submerged in a 2 K helium bath. The high RRR is needed for the improved thermal conductivity in order to minimize the temperature gradient across the sheet metal keeping the RF current carrying surface at the lowest temperature possible. The cavity was designed for high current operations and the resulting superior HOM damping performance was an important factor in selecting the design for CEBAF.

6.2.9 Cavity Pair

Two cavities are assembled together into a cavity pair (see Fig. 6.3) with the FPCs together at the center of the pair [9]. The cavity pair includes an inner adapter between the cavity flanges, two end adapters at the ends of the cavities, end dishes for interfacing to the helium vessel, vacuum valves, and two PFC extensions between the cavity FPCs and the helium vessel feedthrough plate. All components inside the end adapters are made from niobium. All components are joined using bolted connections with indium wire seals. The center of the cavity pair is fixed and bellows in the end dish assemblies allow for the differential thermal contraction between the niobium cavity pair and the stainless steel helium vessel.

6.2.10 Tuner

The SRF cavities are required to be tuned to 1497 MHz ± 50 Hz during 2 K operation. After cooldown of the cavity the frequency is required to be tuned ±200 kHz to ensure operations at 1497 MHz. The frequency is controlled by a mechanical tuner (see Fig. 6.5) that can stretch or compress the cavity longitudinally changing the resonant frequency. The tuner resolution requirement is 50 Hz. With the cavity frequency sensitivity of ∼200 kHz per millimeter, the resulting mechanical resolution requirement is 25 nm. The tuner attaches to the first and fifth cell of the cavity and is submerged in liquid helium during operation. The tuner is driven by a stepper motor mounted external to the cryomodule that transfers torque through two rotary feedthroughs. The rotary feedthrough connects to a right angle driveshaft. The driveshaft ends in a ball screw that acts to change the length of the tuner active leg. The two cell holders are attached on one side to the active tuner leg and the opposing tuner dead leg. The tuner includes limit switches and hard stops to limit the tuner range and prevent damage to the cavity. Major disadvantages of this design include the requirement for the tuner to be submerged in the helium bath, required rotary feedthroughs on the vacuum and helium vessels, and the backlash as the tuner goes from compression to tension (in later implementation of the tuner the backlash was eliminated by biasing the tune of the cavity and operating the tuner in tension only). Early accelerated life testing was done [10] to qualify the mechanical systems.

6.2.11 Helium Vessel

The helium vessel has several major functions in the CM design. The first is to house the cavity pair in a bath of liquid helium. This requires the vessel to be leak tight and

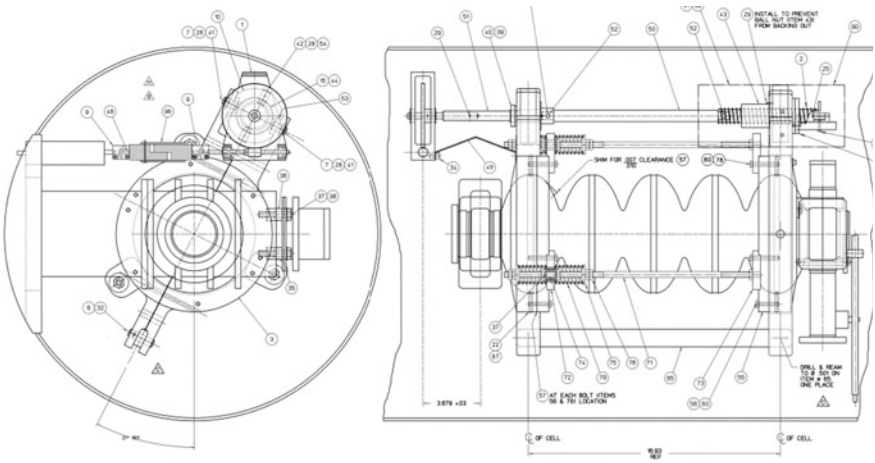

Fig. 6.5 C20 cavity frequency tuner

operate over a range of temperature from 350 to 2 K. The second is to provide the required feedthroughs for RF power, instrumentation, and tuner mechanical drive to the cavity pair. Additionally, the helium vessel provides the support structure for the cavity pair inside the cryostat. The body of the helium vessel is a 24 in outer diameter cylinder with a massive feedthrough plate. The entire assembly is made from 316L stainless steel. The feedthrough plate is a thick plate to provide a stable interface for the waveguide indium seals, instrumentation metal gaskets seals, and welded rotary feedthrough connections. After inserting the cavity pair inside the helium vessel body the waveguide indium seals are made up and the end dish assemblies are welded to dished heads that bridge the end dishes to the helium vessel body closing the assembly. The dished head assemblies include mounting supports and a 4 in. upper and 0.75 in. lower helium connection. The mounting supports accommodate four nitronic rod on each end that spa from the vacuum vessel to the helium vessel. The large helium connection provides the cross sectional area required for heat and mass transport from one helium vessel to the next and the lower connections maintains constant liquid level throughout the four helium vessels in the CM.

6.2.12 Input Coupler

The CEBAF cryomodule uses a waveguide RF fundamental Power Coupler (FPC). The FPC consists of a warm RF vacuum window that provides a hermetic seal between the RF distribution system air filled waveguide and the cryomodule vacuum waveguide, a warm waveguide assembly, a warm to cold waveguide transition [11] and a cold RF window that provides a hermetic seal between the cryomodule waveguide vacuum and the cavity vacuum. The waveguide vacuum space between the warm and cold RF windows is monitored for vacuum, arcing, and heating. The warm to cold transition waveguide assembly is a thin stainless steel rectangular waveguide with two bellows, stiffening rings for the vacuum load, a shield heat station, flanges on each end, and is copper plated on the inside. The assembly is optimized for a nominal 1500 MHz RF power of 5 kW. This determines the thickness of the copper plating and the location of the thermal intercept. As the RF power increases the optimum position for the intercept moves toward the cold end of the waveguide. The bellows are three convolutions made of thin stainless steel and located close to the ends of the waveguide. The bellows makes up for any slight misalignment between the helium vessel feedthrough plate to the sheet metal cavities. Additionally, the thin walled bellows create a thermal break in the waveguide wall. The FPC contributes 0.8 and 5.5 W to the 2 and 40 K heat loads respectively.

6.2.13 HOM Loads

The LE5 cavity selection for use in CEBAF was partly due to the excellent HOM damping of the cavity and HOM loads. The HOM loads are assembled on the end

of a superconducting waveguide that is mounted on the cavity pair and remains inside the helium vessel. For the CEBAF beam currents the dissipated power in a HOM absorber is a fraction of a watt making it preferable to dissipate the HOM power in the helium bath rather than bringing the heat to the shield or room temperature. The size, both cross section and length, of the waveguide is such that the higher frequency HOM RF power is transmitted to the loads while the fundamental power is cutoff and does not propagate to the HOM load. The simple design of a cutoff waveguide has many advantages for fabrication and assembly. The HOM load material is a particular challenge and was the subject of an extensive development program [12].

6.2.14 Magnetic Shields—Inner and Outer

There are two passive magnetic shields in the cryomodule. One located on the outside of the helium vessel which operates close to 2 K and a warm shield just inside the vacuum vessel that operates at room temperature. Both shields are made from the same high permeability shielding material $\sim$0.01–0.02 in thick. Efforts are made to minimize the holes, joints, or other features that may allow magnetic field into the cavity location. Joints are made with overlaps and taped to ensure minimum leakage in the shield. Considerable effort is given to the details of the mechanical design as any cold working of the material during assembly can degrade the performance. The shield around the exterior of each helium vessel is joined with bridging material extending to the next helium vessel forming a continuous cylinder down the length of the cryomodule that is capped at each end at the end can end plate. Subsequent designs have used segment shields that have end caps after each cavity. These segmented designs provide improved shielding performance. Penetrations from the warm to cold parts of the cryomodule require holes in the shielding. The waveguide penetrations to the cavities are a particularly difficult area to shield as the waveguides themselves have a significant cross sectional area. Extensions can be used to help attenuate the field leakage around a hole in the shielding and should be used where possible. Significant effort was made to eliminate any magnetic material inside the magnetic shielding. The use of 316L stainless steel was required inside the vessel and 304 stainless steel was permitted outside of the magnetic shielding.

6.2.15 Thermal Shield and Multilayer Insulation

Multilayer insulation (MLI) is comprised of alternating layers of thin aluminized Mylar and a low thermal conductive spacer material. MLI is used between the helium vessel and thermal shield and between the thermal shield and vacuum vessel. A nominal 15–30 and 45–60 layers are used respectively. MLI is used to

reduce the radiative heat load to the cryogenic circuits and to reduce the heat flux to the 2 K circuit in the case of a catastrophic loss of insulating vacuum. A copper sheet metal thermal shield is located between the 2 K and room temperature surfaces. The shield is cooled by a single straight line running the length of the cryostat. The thermal shield acts to intercept radiative heat load and is connected to all warm to cold transitions to intercept conduction heat loads.

6.2.16 Vacuum Vessel

The vacuum vessel serves multiple functions in the cryomodule. The 304 stainless steel vessel is the boundary of the insulating vacuum, the support structure for the helium vessels, and provides penetrations for the RF power coupler waveguides and instrumentation feedthroughs. The vacuum vessel is a cylinder with weld flanges on both ends and a large access port aligned with the helium vessel feedthrough plate. Mounted on each weld flange are supports for the nitronic rods that connect the vacuum vessel and helium vessel as a low thermal conducting structural support. The access port is closed with a Top Hat assembly that has provisions for the RF power waveguides, cavity tuner mechanical drives, RF signals, and instrumentation feedthroughs. The Top Hat area contains almost all of the penetrations through the insulating vacuum shell.

6.2.17 Cryounit

The CEBAF Cryounit (CU) is the assembly of the helium vessel, power couplers, instrumentation and vacuum vessel around a cavity pair (see Fig. 6.6). A layer of magnetic shielding and MLI are assembled onto the outside of the vessel. This is inserted into the vacuum vessel which has the thermal shield and MLI preinstalled. The helium vessel is support by four nitronic rods on each end configured in a double x pattern for alignment purposes. Two additional longitudinal nitronic restraint rods are installed to complete the installation. The nitronic rods are used to rough align the cavity flanges to the center of the vacuum vessel and tensioned to set the load on the rods for maintaining the cavity position during and after cool-down. The Vacuum vessel access port is used to install the FPC warm to cold waveguide extensions along with thermal straps and instrumentation wiring. A aluminum “Top Hat” closes the access port and has warm waveguide and window assemblies installed. The warm waveguides are connected to a vacuum manifold allowing a single ion pump to support two FPCs. This assembly maintains the hermetic seal of the cavity pair and is the building block for the cryomodules. Four CU are assembled together in a cryomodule.

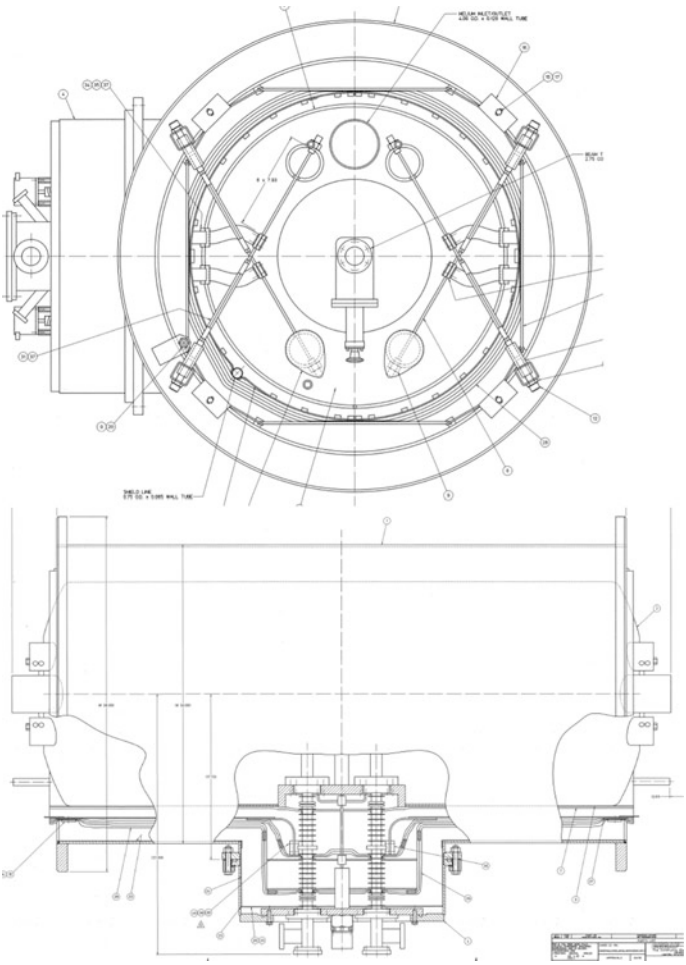

Fig. 6.6 CEBAF C20 cryounit

6.2.18 Instrumentation

The cryomodule cryogenic instrumentation includes temperature sensors, helium liquid level probes, helium bath pressure transducers, vacuum gauges and pumps, and a J-T actuator that is driven with a 24 VDC motor and the valve position is monitored with LVDTs. The temperature sensors are silicon diodes with $\sim 1/4$ degree accuracy. In operation the absolute accuracy of the temperature sensors has not been important as these are primarily used for controlling cooldown where rate of change is important for identifying off-normal conditions like a degraded insulating vacuum that produce large changes in temperature. The liquid level probes used are a superconducting wire type. It is important to adjust the excitation current

to the operating conditions as the helium pressure changes the cooling on the superconducting wire. Warm capacitance manometer pressure transducers are used for pressure measurement. The connection of the pressure transducer to the helium bath should keep the 2 K heat load small while trying to maximize the conductance from the bath to the transducer. In the C20 design the annual space of the return bayonet is used for this connection. This adds no heat load to the system but does limit the conductance and associated bandwidth of the measurement made possible with the connection. The waveguide vacuum space is monitored for RF heating using an infrared sensor mounted inside the waveguide vacuum and isolated from the RF by a cutoff tube, RF discharge with a photomultiplier tube mounted outside the vacuum space through a transparent window mounted on a metal seal flange, and vacuum discharge using a 20 L per second ion pump. Additional vacuum monitoring is done for the insulating vacuum using a cold cathode gauge and the beamline using a 30 L per second ion pump. The waveguide instrumentation is used in the RF interlock chain while the beamline ion pump is used in the RF and beamline valve interlock chains.

6.2.19 Final Assembly

The cryomodule is made up from six major components, four CUs and two end cans. The CUs and end cans are assembled onto a rail where they are aligned in x and y as well as longitudinally. The location of the end cans is tightly controlled. This along with the careful control of the cryogenic distribution system allows for the use of standard size u-tubes avoiding the need for custom fabrications. The CUs and end cans are assembled with a set of "bridging" components. Each bridging section between the components has the helium circuits connected with welded connections and the MIL, thermal shield, and magnetic shields are extended, and insulating bridging ring is positioned and welded in place. The final alignment of the cavities is done by adjusting the nitronic rods which are accessed through small o-ring sealed ports located on each bridging ring.

6.2.20 Status

The first C20 cryomodule was installed in the CEBAF tunnel in 1990 and the machine was completed in 1993. Since that time the cryomodules have performed well above their design parameters. The original 5 pass energy of 4 GeV was exceeded and 6 GeV operations was achieved with the original cryomodules. Since that time there has been a slow degradation in gradient performance of some cryomodules. As a result a refurbishment program was initiated. The progress with cavity processing in the intervening time allowed the performance specification for cavity gradient to be increased to 12.5 MV/m. This results in a "C50" cryomodule

with 50 meV energy gain per cryomodule per pass. Along with the increase in cavity performance some designs were improved during this work. The FPC waveguides had a newly designed "dogleg" section installed eliminating flashover on the ceramic RF window and the tuner mechanical coupling was modified to eliminate twisting and resulting backlash in the drive train. To date eleven cryomodules have been refurbished and the twelfth is in process.

6.3 The Spallation Neutron Source (SNS) Cryomodule

6.3.1 Introduction

The SNS is a 1 GeV negative hydrogen ion accelerator with up to 2 MW power producing a source of neutrons for materials research. The initial portion of the acceleration is achieved via a conventional negative proton injector, a drift tube linac (DTL) and a coupled cavity linac (CCL), that provide a nominal energy gain up to 185 MeV. The machine was changed in December 1999 from a warm temperature to a cold temperature linac to improve overall machine performance. The super-conducting linac (SCL), discussed here, contains 11 medium beta cryomodules capable of 345 MeV and 12–21 high beta cryomodules capable of up to 1300 MeV. After passing through an accumulator ring the beam goes to a mercury target where a neutron beam of as much power as 2 MW is produced.

The cryomodule (CM) is based on the CEBAF CM with improvements borrowed from LHC, TESLA, and the JLab 12 GeV upgrade and uses the frequency scaled KEK fundamental power coupler (FPC). Figure 6.7 is the elevation view of the high beta CM, while Fig. 6.8 is the flow schematic. The FPC requires a 4.5 K lead flow to cool the outer conductor; therefore the LHC concept of producing the 2 K in the CM rather than in the refrigerator is utilized.

The refrigerator produces a 3 bar, 4.5 K stream, which feeds two Joule-Thomson (JT) valves in parallel. The first supplies a small sub-cooler in the CM and then cools the cavity. The second feeds the power coupler outer conductor. The CM

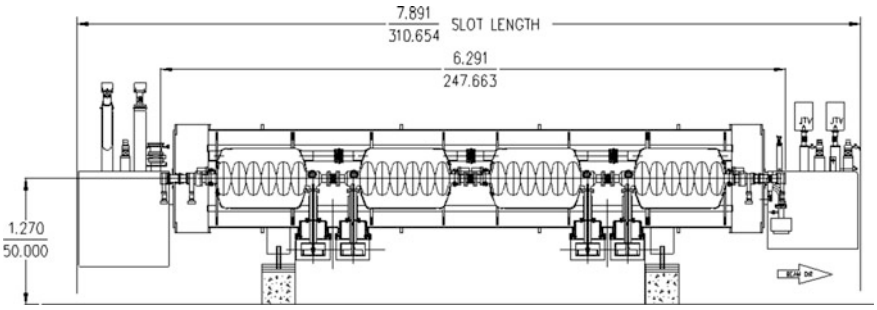

Fig. 6.7 High beta cryomodule schematic

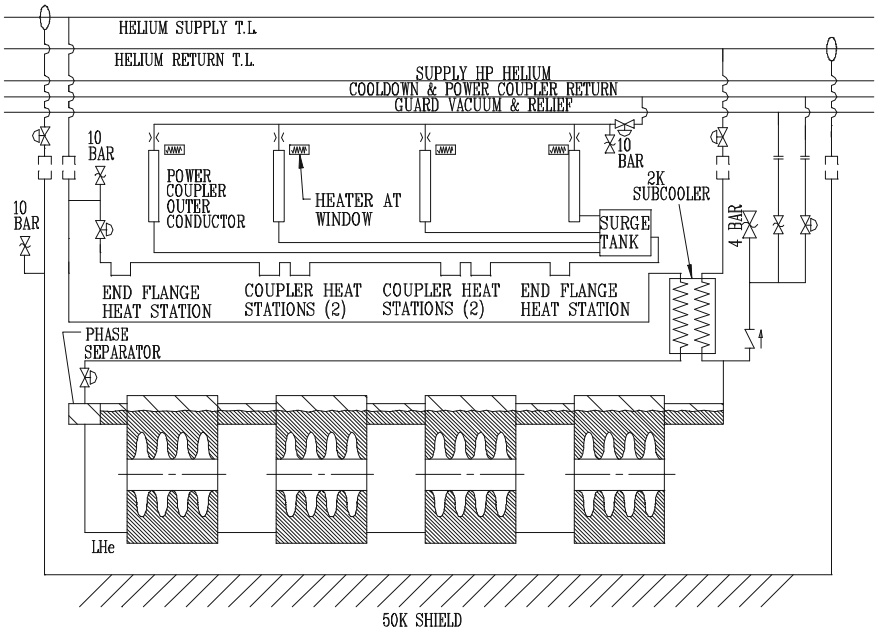

Fig. 6.8 Flow schematic

shield is cooled by a 4 bar, 35 K stream, which first cools the supply transfer line (TL) shield, then the CM shield, and finally the return TL shield before returning to the refrigerator at 52 K. The bayonet design permits replacement of a CM in less than a day if needed without warming up the entire linac. In the nine years since the initial CEBAF cooldown, the linacs have never been warmed up and only four CMs have been replaced during scheduled accelerator shutdowns.

The relevant parameters for both medium and high beta CMs are given in Table 6.2 and the relevant refrigeration capacities are given in Table 6.3.

6.3.2 Cavity String

The design, manufacture, and performance of the SRF cavities are reported elsewhere [13]. The medium beta CM consists of three six-cell cavities while there are four six-cell cavities for the high beta CMs. The SNS cavities operate at 805 MHz. During initial cold tests, the cavities have met the design requirement for accelerating gradient, which is an E_{peak} of 27.5 MV/m at a design quality factor, Q_0, of 6×10^9 at 2.1 K. Power dissipation per cavity at 7 % duty cycle is 2 and 3.5 W for the medium and high beta cavities respectively. The relationship of Q_0 with temperature follows BCS theory. Accordingly, the Q_0 of 14×10^9 at 2 K decreases to 6.9×10^9 at 2.3 K. The two different beta cavities are elliptical in shape,

Table 6.2 SNS cryomodule parameters

	Medium	High
Slot length	5.839 m	7.891 m
CM length (bore tube)	4.239 m	6.291 m
CM diameter	1.22 m (∼48″)	
2 K Heat load (static/dynamic)	25/14 W	28/20 W
Maximum coupler flow		0.075 g/s
Shield heat load including Transfer Line	170 W	200 W
Tunnel H × W		10 × 14 ft
Control valves per CM		5
Bayonets per CM		4
Radiation hardness		10^8 rads
Pressure rating	2 K System Warm	3 atm
	Cold	5 atm
	Shield and 4.5 K systems	20 atm

Table 6.3 Refrigeration capacities

	He temp (K)	Capacity (W)	Pressure (atm)	Flow (g/sec)
Linac shields	35–52	8300	4.0	90
Linac cavities	2.1	2400	0.041	120
Secondary	4.5		3.0	0.15

manufactured from 4 mm thick niobium and have stiffening rings at 80 mm to minimize microphonics. The performance of the first prototype medium beta cavity, shown in Fig. 6.9, exceeded the required performance.

The cavities are housed in a titanium helium vessel, which matches the coefficient of thermal expansion of the cavity. The cavity is maintained at operating frequency through a TESLA-style tuner mounted on one end of the helium vessel, which operates through a bellows. The tuner, manufactured out of stainless steel, is actuated through a cold stepping motor through a harmonic drive. Power is brought into the cavity through the coaxial FPC [14] at one end of the cavity. Higher order mode extraction filters are attached at each end of the cavity to damp some potentially dangerous longitudinal modes. The string of cavities in the helium vessel with couplers, HOM damping filters and hermetic valves are assembled in JLab Class 100 clean room to minimize contamination. Figure 6.10 shows the arrangement of the cavity string including the cavity, coupler, helium vessel and tuner.

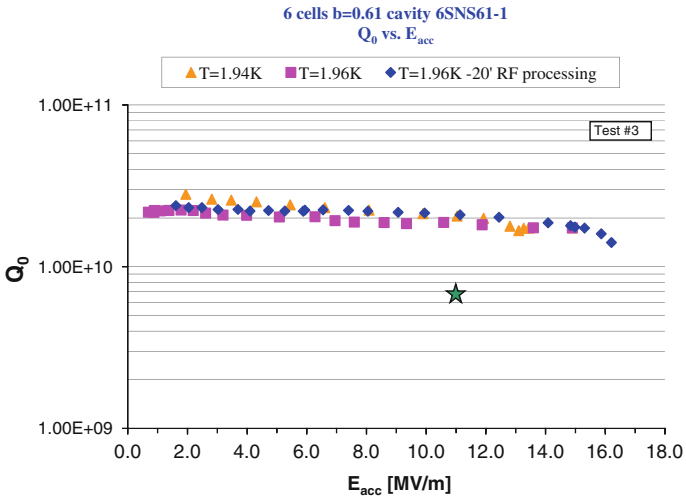

Fig. 6.9 Medium beta cavity performance

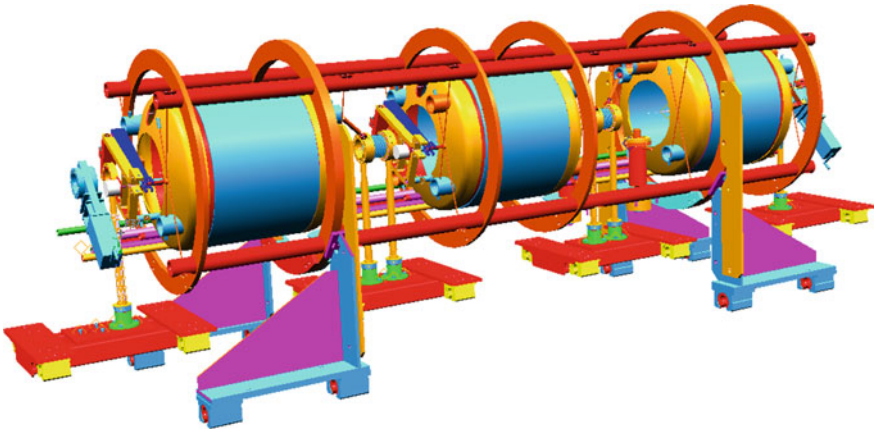

Fig. 6.10 Cavity string components inside the space frame situated on tooling

6.3.3 Cryomodule

A high beta CM consists of two end cans, a vacuum tank, a space frame, a thermal shield, two magnetic shields and a hermetically sealed string of four cavities in the helium vessel each with FPCs, a field probe, two HOM filters, bellows between cavities and seal valves. A medium beta CM is similar in construction but houses a string of three hermetically sealed cavities instead of four. The general arrangement of these components is shown in Figs. 6.11 and 6.12. The CMs used in CEBAF, the

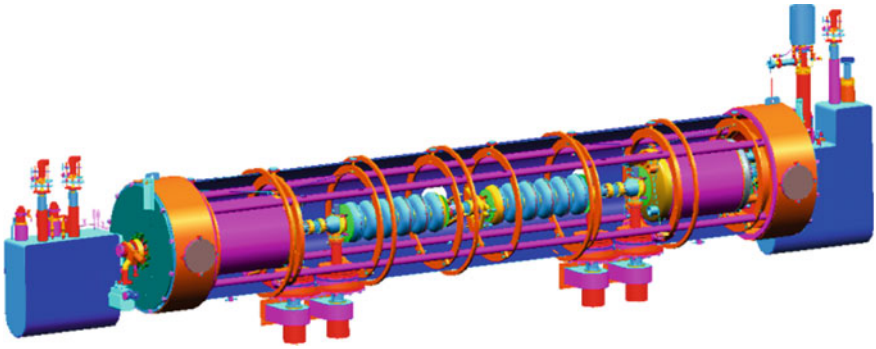

Fig. 6.11 High beta cut-away

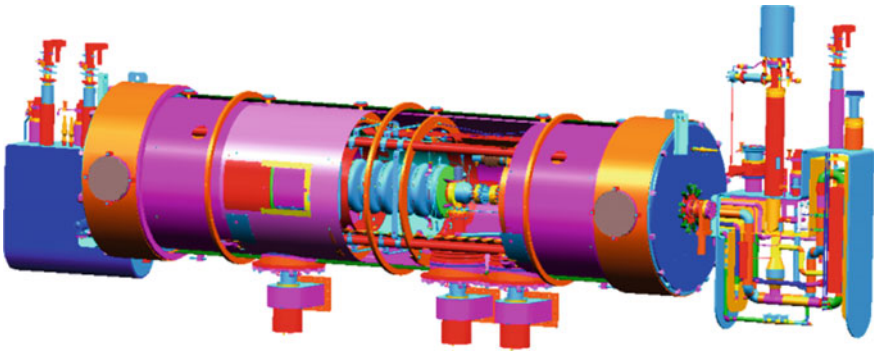

Fig. 6.12 Medium beta cut-away

largest use of SRF in the US, employs a similar construction arrangement. What makes the SNS design unique is that the CMs are assembled at JLab and shipped to the SNS site at Oak Ridge National Laboratory (ORNL). This led to the development of a structure that can handle the over-the-road shipment of 500 miles while maintaining alignment of the cavities in a low loss cryostat [15]. The space frame was developed at JLab for the next generation JLab CM to facilitate installation of long strings of cavities efficiently at a relatively low cost. The space frame was adapted and strengthened to handle the relatively high transportation loads incurred during shipment to ORNL. The vacuum tank provides a support structure for the space frame and minimizes the gaseous conduction to the cold surfaces on the cavity string. The string is supported off of the space frame through nitronic rods, which limit the solid conduction between room temperature and the cryogenic surfaces. These rods are also able to take the shipping loads and maintain the cavities in alignment. A thermal shield, operating at 50 K, surrounded with multilayer insulation (MLI) provides a radiation barrier between the cavities and the outside world. There are two magnetic shields, one outside the space frame and the

other at the helium vessel, which in concert reduce the earth's and stray magnetic fields by a factor of ~100 to minimize the effect on the cavity Q_0. L shaped end cans, a design developed for CEBAF to save space, close off the cavity string in the vacuum tank and provides the interface for the helium to cool the cavities, the couplers and the thermal shields. Between each CM is a 1.6 m warm space that contains quadrupole magnets and diagnostics including beam position monitors, current transformers and wire scanners.

6.3.4 Cryomodule Heat Loads and Thermal Design

The design parameters for the CM were developed in conjunction with the design parameters for both the cryogenic system and the SC portion of the linac and are given in Table 6.2. Specifically, the heat load budgets were developed considering operational experience with the CEBAF cryogenic system, where applicable. The heat load estimates and the budget for the CM are given in Table 6.4. This section contains a summary of the heat loads as well as detailed descriptions of the contributions of each subsystem.

6.3.4.1 Cavity, Helium Vessel and Tuner

The SNS helium vessel design, described in [16], supports the cavity during all phases of operation, facilitates cavity tuning and contains the cryogens with appropriate plumbing. Each 0.61 m diameter titanium helium vessel contains a single niobium cavity whose six cells are immersed in ~150 L of He-II during normal operation. The ends of the cavities protrude through the helium vessel heads into the insulating vacuum to allow beamline assembly as well as attachment of FPCs, Higher Order Mode (HOM) filters and field probes. These end groups are subject to radiation heat transfer from the 50 K shield and the FPC, solid heat conduction from instrumentation leads and the FPC as well as power generated within the HOMs. Extraction of HOM signals to room temperature is planned, requiring a 3.6 mm semi-rigid coaxial cable running from the cavity to the vacuum tank exterior. Based on finite element analysis, the heat loads incident on the HOMs must not exceed 0.25 W in order to maintain the HOMs well below the niobium critical temperature. Additionally, instrument wiring for temperature diodes, liquid level sensors, and heaters are routed from the helium vessel to the vacuum tank exterior. The helium vessel heads possess attachment points for Nitronic-50™ stainless steel support rods and the cavity tuner. The calculated heat load intercepted by the cavity and helium vessel assembly is given in Table 6.4.

The dynamic heat load for each cavity design has been calculated for E_{peak} = 27.5 MV/m. It is desirable to increase the accelerating gradient such that E_{peak} = 35 MV/m, thereby reducing the number of high beta cryomodules required

Table 6.4 Calculated heat loads (W) for the medium and high β cryomodules

Estimate summary		MBCM			HBCM	
	Qty	2.1 K	50 K	Qty	2.1 K	50 K
Static—(see itemized list)	1	9.7	131	1	11.5	161
U-Tube Allotment	1	10.0	24	1	10.0	30
Dynamic (see itemized list)	1	8.3		1	17.1	
Total heat load per CM		28.0	155		38.6	191
Budget per CM		39.0	170		48.0	200
Dynamic contributions						
Cavity	3	6.0		4	14.0	
Power coupler	3	0.6		4	0.8	
Bellows	2	0.2		3	0.3	
HOM (2 per cavity)	3	1.5		4	2	
Total dynamic		8.3			17.1	
Static contributions						
Radiation—HV and bellows	3	1.1	41.7	4	1.8	65.3
Power coupler (radiation)	3	2.1		4	2.8	
Tuner	3	0.75		4	1	
He vessel supports	3	0.2	18	4	0.3	24
Warm beam tube conduction	2	0.1	2	2	0.1	2.5
Warm beam tube radiation	2	0.9	0.9	2	0.9	0.9
Cables (3 per cavity)	1	0.5	1.8	1	0.5	1.8
Supply bayonets	2	1.0	12	2	1.0	12
Radiation	1	0.04	9.0	1	0.04	9.0
PC J-T valve	1	0.25	2	1	0.25	2
Subcooler J-T valve	1	0.25	2	1	0.25	2
Shield relief	2	0.0	4	2	0.0	4
5 K transfer line	1	0.1		1	0.1	
50 K transfer line	1		3	1		3
Return bayonets	2	1.5	6	2	1.5	6
Radiation	1	0.1	11.2	1	0.1	11.2
Cooldown/PC return	1	0.25	10	1	0.25	10
Shield relief	1	0.3	2	1	0.3	2
Cooldown valve	1	0.25	2	1	0.25	2
5 K transfer line	1	0.0		1	0.0	
50 K transfer line	1		3	1		3
Total static		9.7	131		11.5	161

to reach a given linac output energy. The dynamic heat load increases at least quadratically with increasing peak gradients or higher if operated in the field emission region. These increased losses would be handled by some portion of the available margin in the primary circuit of the refrigeration system.

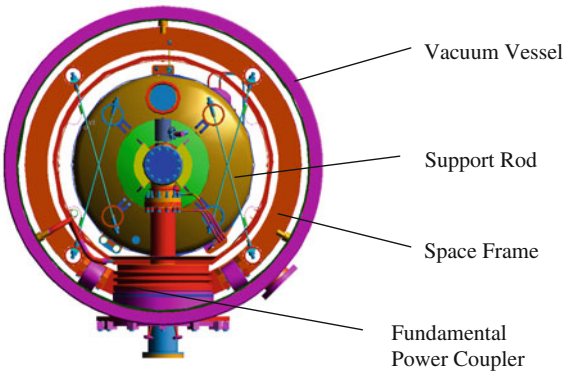

Fig. 6.13 Nitronic-50™ support rods attach the helium vessel assembly to the space frame

6.3.4.2 Vacuum Vessel and Space Frame

The vacuum vessel and space frame, described in [17], serve to locate the cavities accurately within the CM via the Nitronic-50™ support rods, provide the structural links to the external supports and remain at room temperature (300 K) during normal operation (Fig. 6.13). The 0.99 m diameter vacuum vessel contains the insulating vacuum and provides pressure containment in the unlikely event of cryogenic piping failure. The insulating vacuum is cryo-pumped during accelerator operation to less than 1.3×10^{-9} atm, an adequate vacuum level to minimize residual gas conduction. If a cryogenic piping failure occurs, two spring-loaded parallel plate pressure reliefs, identical to those used in the CEBAF CM, open at 1.2 atm on the vacuum vessel. In addition, there are many flanged penetrations in the vacuum vessel: ports in the bottom of the vacuum vessel through which the FPC provides RF power to the cavities, instrumentation ports containing electrical feed-throughs for diodes, cavity heaters, tuner power and limit switches, field probes, and connections for the warm helium coupler exhaust.

6.3.4.3 Thermal Radiation Shield

As in CEBAF, a copper shield, 2.37 mm thick, operating between 35 and 50 K is used to intercept thermal radiation (Fig. 6.14). The shield is cooled by supercritical helium gas (4 atm, 35 K) through a single pipe, 22.2 mm outer diameter by 1 mm thick wall. Thermal analysis of both single-pass and three-pass shield cooling showed ~ 2 % increase in the total static heat load to 2 K with a single-pass cooling scheme. Cost ultimately dictated the choice of single pass versus three-pass piping.

The shield is divided into segments that cover the helium vessel assemblies and bridges that cover both the cavity-cavity and cavity-end-can interconnect regions. The bridge sections allow access to the cavity string for assembly, alignment, instrumentation wire routing and tuner maintenance. There are three segments in a

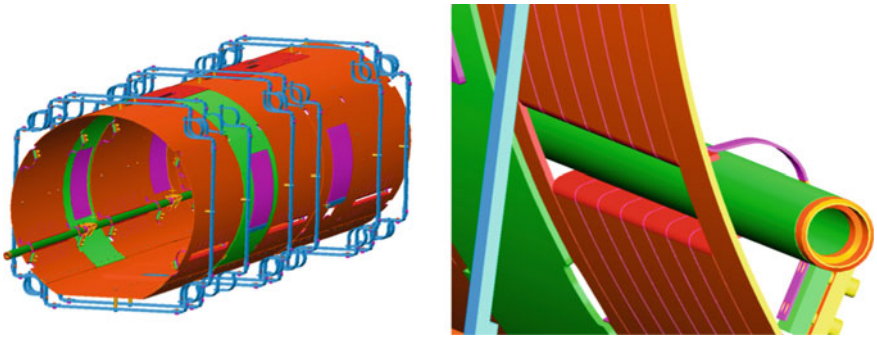

Fig. 6.14 MBCM thermal shield assembly (*left*) and piping strain-relief (*right*)

medium beta cryomodule and four segments in a high beta cryomodule. A hydro-formed stainless steel bellows, soldered with EasyFlo-45™, connects the copper piping between segments. In addition to the bellows, a series of tabs 76 mm long × 76 mm wide, where the pipe is soldered with BCuP to the shield, provides strain relief from differential thermal contraction of the piping and shield during cool down and operation.

The horizontal and vertical helium vessel Nitronic-50™ support rods are heat-stationed to the shield segments by copper straps, 1 mm × 25 mm × 125 mm long. All wiring and cabling routed to 2 K is heat stationed at 50 K on the nearest shield segment as well. Due to the long length (>600 mm), small cross-sectional area (20 mm^2) and difficulty during assembly, the two axial support rods are not heat stationed. The additional heat load to 2 K is negligible (<1 mW/support).

Each bridge is fixed at only one end to an adjoining segment with PEM fasteners and allowed to slide over the other neighboring segment. Each segment-bridge assembly weighing ∼45 kg is supported by eight G10 straps, 38 mm × 4.8 mm × 508 mm long, terminated with stainless steel pipe clamps affixed to the space frame support tubes. The four horizontally oriented supports react lateral shipping and handling loads, the four vertically oriented supports react both gravity and transportation loads and all eight react any axial loads.

6.3.4.4 Multilayer Insulation (MLI)

The insulation system design is identical in principle to that employed in the original CEBAF CM and is expected to achieve the same thermal performance. The insulation scheme reduces the radiative heat load to the cold surfaces, provides ample mass and heat capacity to mitigate thermal transients and is comprised of materials suitable for use in a high radiation environment.

Blankets are constructed of alternating layers of double-aluminized Mylar™ (DAM), 25 μm thick, and Reemay™ #2250, a spun-bonded polyester 75 μm thick. The maximum emissivity allowed by emissometer measurement is 0.035 at room

temperature. The surfaces of the helium vessel are covered with two 12-layer blankets, the beamline components and piping are spiral-wrapped with 15 layers at a 50 % overlap, and the 50 K surfaces are covered with four 15-layer blankets. The joints and seams, staggered both axially and around the circumference by 25–50 mm, are closed with 25.4 mm wide aluminized Mylar™ tape.

Effective thermal conductance through the blanket layers is calculated considering three mechanisms: radiative heat transfer—governed by emissivity (ε) and geometry, solid conduction—governed by effective thermal conductivity (k_{eff}) and geometry, and residual gas conduction—governed by average local pressure. A Fortran program, TRANSAM, written originally for transfer line design was used to estimate the expected heat flux to the 50 and 2 K surfaces. Using a worst-case scenario with average pressure of 10^{-4} torr, $\varepsilon = 0.2$ and $k_{eff} = 1.5$ mW/cm K, the heat flux to the 50 K thermal shield was calculated conservatively as 2.5 W/m^2. Using the same average pressure, $\varepsilon = 0.06$ (lowered since emissivity typically decreases with decreasing temperature) and $k_{eff} = 1.5$ mW/cm K, the heat flux to the 2 K surfaces was calculated to be 94 mW/m^2. While these values are conservative, proper assembly and installation of the blankets is required for ideal performance. Taped joints, insufficient overlap and compaction of blanket layers can reduce the effectiveness of the MLI thereby increasing significantly the incident heat load. Combining the realities of assembly with the fact that nine of twenty-two measured CEBAF CMs, as reported in [18], exceeded the 50 K static heat load design criteria, it was decided to increase the estimated radiation heat load to 200 % of the calculated values.

6.3.4.5 End Cans, Heat Exchanger and Cryogenic Piping

The end cans route helium to and from the CM, provide controls for the primary and secondary circuits, provide beamline vacuum connections and contain pressure relief valves used in the event of loss of vacuum (Figs. 6.11 and 6.12). The end cans use bayonet connections that are identical to those used in the CEBAF CM [19]. In addition to the primary and shield supply bayonet connections, two J-T valves similar to those used in CEBAF are installed in the supply end can: the primary J-T has a $C_v = 0.3$ and the secondary J-T has a $C_v = 0.05$. The return end can contains a sub-atmospheric primary return bayonet, the shield return bayonet, a Circle Seal™ pressure relief valve plumbed in parallel with a parallel plate relief valve, a cool-down valve with a $C_v = 3.0$ and a helium-helium heat exchanger (HX).

The counter flow HX (Fig. 6.15) is a plate-fin type core constructed of aluminum with a pressure rating of 12 atm. Stainless-to-aluminum joints transition from the aluminum body to the stainless steel process piping. The design parameters are given in Table 6.5. Silicon diodes are installed in the assembly to measure HX terminal temperatures in order to assess the HX effectiveness.

The stainless piping within the CM is strain-relieved from the end can connections with flexible metal hose. All of the shield circuits, the fill-lines between

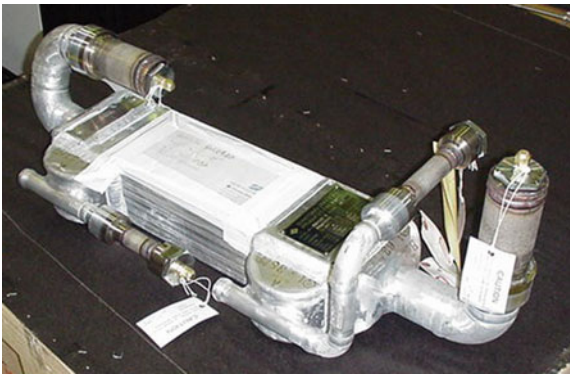

Fig. 6.15 Helium-helium heat exchanger

Table 6.5 Heat exchanger design parameters

	High pressure side	Low pressure side
Core length	600 mm	–
Core cross section	100 mm × 100 mm	–
Maximum allowable helium leak rate	1×10^{-9} mbar l/s external 1×10^{-4} mbar l/s cross-passage	–
Pipe size	26.7 mm OD × 2.1 mm wall (¾″ IPS Schedule 10)	60.3 mm OD × 2.8 mm wall (2″ IPS Schedule 10)
Maximum flow rate	6.0 g/s	6.0 g/s
Fluid inlet pressure	2.95 atm	0.040 atm
Maximum pressure drop	0.020 atm	0.001 atm
Inlet temperature	5.0 K	2.1 K
Outlet temperature	2.2 K	3.96 K
Capacity	60 W	–
NTU (integrated)	4.37	–
Effectiveness	0.97	–
UA (integrated) and UA margin	93.2 W/K and 20 %	–

helium vessels and the primary circuit plumbing through the HX high-pressure side are 26.7 mm OD × 2.1 mm wall. The primary return piping through the HX and in the relief stack is 60.3 mm OD × 2.7 mm wall, sized for a catastrophic loss of beamline vacuum. The helium vessel return headers are 88.9 mm OD × 3.0 mm wall, and along with the helium vessel provide 10 % ullage. The secondary circuit consists of 6.35 mm outer diameter × 1.3 mm wall stainless steel tubing, sized to reduce helium inventory in that circuit, and a 1 L surge tank which functions to damp potential flow oscillations that may arise during operation.

6.3.4.6 Fundamental Power Coupler

Due to operating frequency and space constraints, a coaxial coupler with inner and outer conductors was selected instead of a waveguide coupler to provide fundamental RF power to the cavities. Besides delivering RF power, the coupler must not adversely affect the electromagnetic performance of the cavity or the thermal performance of the cryomodule. Cavity cleanliness procedures require the coupler to be inserted into the cavity at the six o'clock position.

To handle static and dynamic heat loads in the coupler and cavity, the outer conductor is cooled by a nominal stream of 3 atm, 5 K supercritical helium flowing at 0.038 g/s per coupler and the inner conductor is conduction cooled by a 1 L per minute water flow. The ceramic RF window is maintained at 300 K during operation by a heater-thermocouple control loop.

The outer conductor is a machined and welded stainless steel assembly with flanged connections to the cavity and the warm window. The internal vacuum surface is copper-plated with a nominal thickness of 15 μm and an estimated RRR = 10 to reduce resistive wall losses induced by the RF surface currents. A single helical, square-grooved flow passage, 2.3 mm wide × 1.6 mm deep (Fig. 6.14), with a pitch of 2.6 turns/cm is machined into a thick-walled stainless steel tube, 75.75 mm internal diameter. A thin-walled stainless steel tube (1.6 mm O.D.) is then shrunk-fit over the outer diameter of the flow passages and welded leak tight onto the ends nearest the flanges. Due to the small hydraulic diameter of 2.16 mm, flow velocities and Reynolds number are kept high to mitigate potential deleterious effects of buoyancy, re-circulation and poor heat transfer in the helium stream.

Conduction heat load estimates (Table 6.3) were calculated for the outer conductor using an Excel model that included combined conduction and convection heat transfer as well as temperature-dependent thermal properties for stainless, copper and supercritical helium gas (Fig. 6.16). A separate estimate of the static radiation heat load emitted from the FPC to the beam pipe was calculated.

Fig. 6.16 He gas cooling passages (*right*) and FPC outer conductor assembly (*left*). The helium gas flow rate of 0.038 g/s produces an exhaust temperature of 210 K (*center*)

The values were used as input to a finite element model of the cavity ends to verify that they remain below the niobium critical temperature.

In an effort to determine if thermo-acoustic oscillations or flow instabilities exist in the secondary circuit, a test rig was been designed and built.

6.3.5 *Thermal Performance of the SNS Cryomodule*

6.3.5.1 Budgeted Versus Estimated Heat Loads

For the primary circuit maintained at 2.1 K, the heat loads are divided into three categories: (1) a static contribution consisting of solid conduction, residual gas conduction and radiation, (2) a dynamic contribution consisting of RF heating in the cavity and coupler and (3) a distribution system allotment that consists of u-tube and transfer line heat loads. There is no dynamic contribution to the 50-K shield and its cooling circuit. Details of the estimated heat loads are given in Table 6.3. Budgeted heat loads in contrast, are those that each component are allowed to have and are used in the sizing of the cryogenic refrigeration system. A comparison of the budgeted and estimated heat loads is provided in Table 6.6. For the medium beta cryomodule, the total estimated heat load to the primary circuit is 72 % of the budget per cryomodule, and for the shield circuit is 91 % of the budget per cryomodule. The primary static heat load for the medium beta cryomodule is estimated as 9.7 W and includes contributions from bayonets, valves, supports, wiring, cabling and radiation. The dynamic heat load is estimated as 8.3 W and is divided evenly between the three cavities and FPCs housed within the cryostat.

6.3.5.2 Measured 2 K Static and RF Heat Loads

The following measurement technique, similar to that employed during CEBAF CM acceptance testing [5], is used to quantify the static heat load and RF heat load. With the primary J-T supply valve and u-tube return valve closed, the

Table 6.6 Comparison of heat load budget versus estimate for both SNS cryomodules

	β = 0.61 cryomodule (3 cavities)				β = 0.81 cryomodule (4 cavities)			
	2.1 K		50 K		2.1 K		50 K	
Description	Budget	Estimate	Budget	Estimate	Budget	Estimate	Budget	Estimate
Static	15	9.7	146	131	18	11.5	170	161
Dynamic	16	8.3	N/A	N/A	28	17.1	N/A	N/A
U-Tubes and distribution	10	<10	24	<24	10	<10	30	<30
Total	41	<28	170	<155	66	38.6	200	<191

helium bath pressure rate-of-rise is measured during three conditions: with the helium bath heater on (HEATER), with only RF power on (RF) and with no heater or RF power (STATIC). Five separate 30-second measurements are made in the following order—STATIC, HEATER, STATIC, RF and then STATIC. Using a known heater power (Q_{heater}) and the average rate-of-rise (dP/dt) for each condition, the static and RF heat loads are then calculated from the following equations:

$$Q_{static} = Q_{heater} * \left(dP/dt|_{static}\right) / \left(dP/dt|_{heater+static} - dP/dt|_{static}\right) \quad (6.1)$$

$$Q_{RF} = Q_{heater} * \left(dP/dt|_{RF+static} - dP/dt|_{static}\right) / \left(dP/dt|_{heater+static} - dP/dt|_{static}\right). \quad (6.2)$$

Note that during this measurement, the flow to the secondary circuit for the FPC outer conductors ideally should be maintained constant. Actually the inlet temperature to the CM increases during the two-and-one-half-minute data acquisition cycle. Typically several measurements are taken before opening valves to recover the pressure. Over that time span the inlet temperature can increase by as much as 5–7 K. There is a corresponding rise in the FPC cold flange temperature. This transient temperature more closely reflects the fluid temperature rather than the cold flange temperature since measurements have been made at relatively high gradients without indication of quenches. The helium bath pressure initially is approximately 3 kPa (0.030 atm) and may rise to as high as 4.1 kPa (0.040 atm) during the series of measurements. The actual total pressure rise is primarily dependent on the cavity gradients selected for each measurement.

The measurements are accurate to ±½ W due in part to the accuracy of the capacitance manometer pressure transducer as well as the measured voltage and current on the cavity bath heater. Effects from valve leakage and reduced flow in the supply bayonet have been neglected, which result in conservative heat load estimates. Overall, the static heat load measurements agree well with the estimates; the average static load is approximately 10 W (Fig. 6.17).

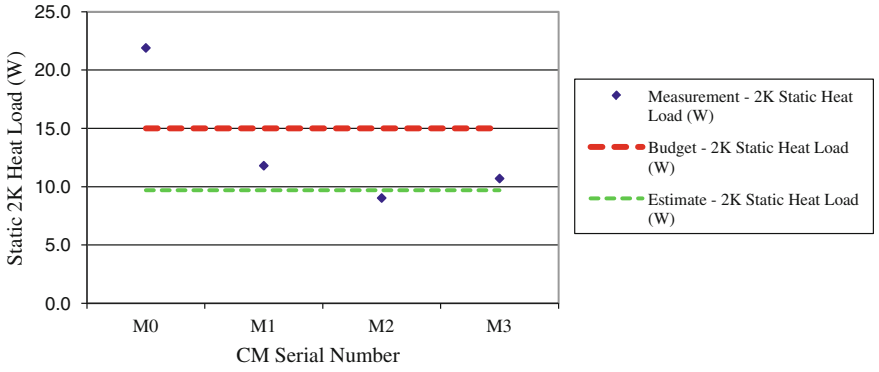

Fig. 6.17 Measured primary static heat load versus CM serial number

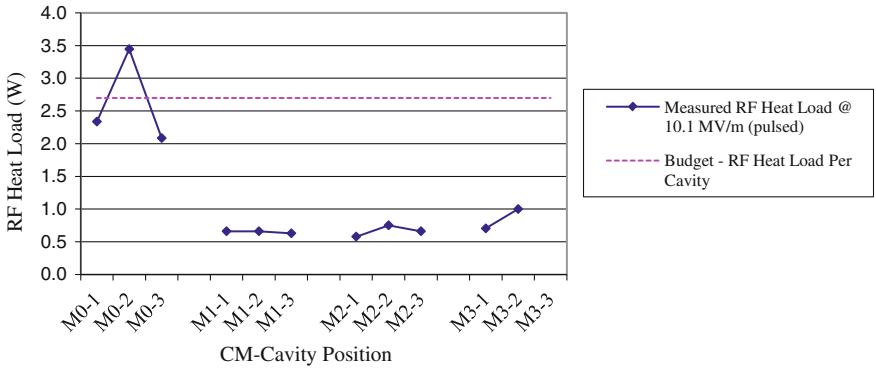

Fig. 6.18 Measured RF heat load versus CM-cavity position at 10.1 MV/m

The measured RF heat load at the required gradient of 10.1 MV/m is approximately equivalent to the estimate for the prototype cavities, 2.7 W, and is less than 1 W for each of the cavities in the three production CMs (Fig. 6.18). One cavity, M3-3, was not measured due to schedule constraints.

The power dissipation scales quadratically with accelerating gradient and is inversely proportional to a geometric factor. For the $\beta = 0.81$ cavities, the required accelerating gradient is 15.5 MV/m and the geometric factor is reduced by 12 %. Assuming no degradation due to field emission, the power dissipation will be approximately two times greater for the higher beta cavities. Initial vertical tests on these cavities have yielded acceptable results.

6.3.5.3 Measured 50 K Shield Heat Load

The measurements of the 50-K shield heat load are in good agreement with predictions (Fig. 6.19). The measurement procedure included the following steps: first for a given valve position, monitor the gaseous helium inlet and outlet temperatures and the mass flow rate, then calculate the heat load using gaseous helium properties and time-averaged temperatures and flow rates. This procedure was repeated at several different flow rates. The accuracy of this type of measurement, approximately ± 10 %, is driven by the helium mass flow meter.

The heat load measured in the prototype CM (M0) is 129 % higher compared with measurements on the production CMs. This is most likely caused by increased residual gas conduction in the insulating vacuum space due to the large helium leak rate that had been detected in the prototype shield process piping after cooldown. The prototype required active turbo-pumping during the entire test period to maintain the vacuum in the range of 10^{-6} torr. In addition, changes in the multilayer insulation blanket design and improved blanket installation techniques contributed to the lower overall heat load in the production CMs.

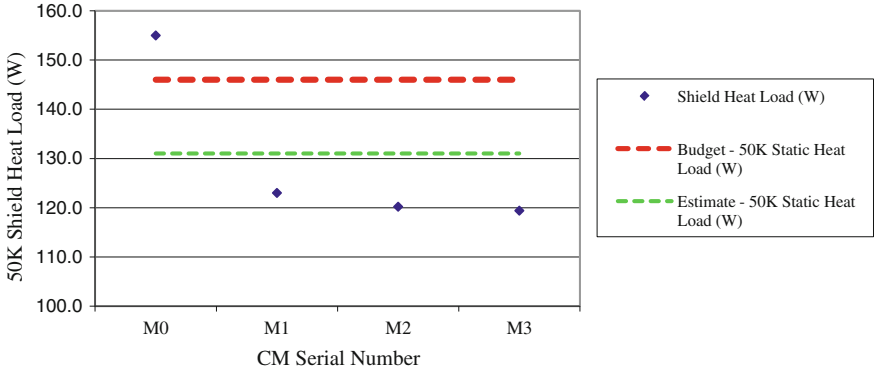

Fig. 6.19 Measured shield heat load versus CM serial number

6.3.5.4 Fundamental Power Coupler Thermal Performance

The primary requirement for the FPC is to transmit a maximum of 550 kW of RF power at a 7 % duty cycle. Adding a 10 % engineering margin, the design goal for the average power handling capability became 53 kW. Another important requirement is to insert the coupler from the bottom to minimize particulate introduction and generation in the cavities. The outer conductor has counterflowing helium-gas cooling to intercept the static and RF heat loads. The maximum flow rate is 0.075 g per second per coupler. The flow passages are sized to keep the flow velocity high enough to overcome buoyancy forces and potential flow instabilities.

To verify the design and confirm the thermal calculations, the FPC installed on the M0-2 cavity was instrumented to measure the temperature profile along the outer conductor. In addition, the exhaust helium mass flow rate was measured during this particular test to determine the maximum power handling capability of the FPC. With a stub tuner installed, the FPC transmitted 9 kW of CW power to the cavity. The resonant condition created by the stub tuner settings resulted in a transmitted power equivalent to 100 kW within the FPC, nearly double the design goal.

The thermal model used the cold and warm end temperatures, the helium mass flow rate and the equivalent transmitted RF power during the test as inputs. The results from the thermal model agree well with the experimental temperatures (Fig. 6.20). The calculated conductive heat load transmitted to the cavity from the outer conductor during the higher power operation was estimated as 1.1 W—the expected conductive heat load at nominal operating conditions is less than 0.25 W.

6.3.5.5 Helium Heat Exchanger Performance

The HX is located in the CM return end can to increase overall cryogenic system efficiency. This enables the SNS supply transfer lines to contain 5-K supercritical

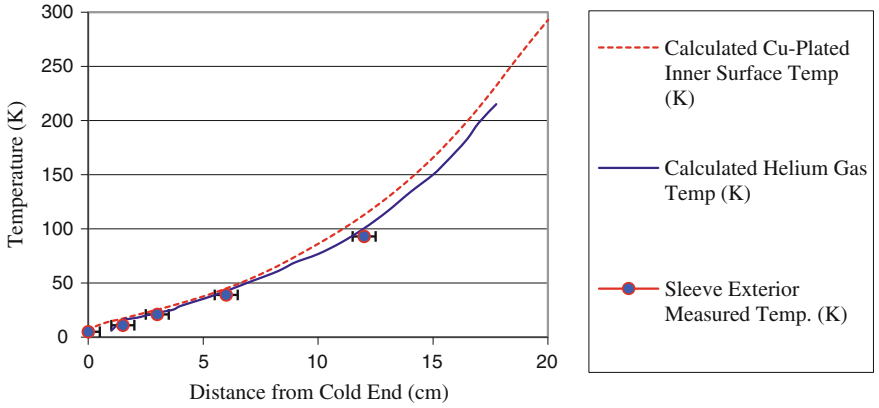

Fig. 6.20 Comparison of analytical and measured temperatures on the M0-2 FPC outer conductor

helium as compared with ~3 K for the CEBAF machine. The HX, a brazed-aluminum plate-fin construction, pre-cools the helium upstream of primary JT valve to increase liquid yield. The effectiveness is specified as greater than 90 % for the design capacity of 60 W. The overall thermal conductance (UA) and number of transfer units (NTU) are 93.2 W/K and 4.37, respectively. The assembly is required to be leak tight to 1×10^{-9} mbar l/s.

Initial measurements indicate that the performance is consistent with estimates. The measured inlet and outlet temperatures on the low-pressure-side of the HX are 2.0 and 3.5 K respectively, compared with estimates of 2.1 and 3.96 K. Inlet and outlet temperatures for both streams are required to calculate the effectiveness of the counter-flow HX. Since the high-pressure-side inlet temperature indication is not reliable due to the placement of the silicon-diode temperature sensor, the effectiveness has not been calculated.

6.3.5.6 Conclusions on the Thermal Performance

Measurements of thermal performance have been completed on the prototype and three production CMs. Results obtained for the static, RF and shield heat loads are in good agreement with estimates and are within budgeted heat loads. Measurements of the outer conductor thermal profile are in good agreement with calculations and indicate that the heat load from the FPC is acceptable. The FPC and its outer conductor can transmit approximately two times more than the required maximum RF power expected from the SNS klystrons. Initial measurements of the available heat exchanger terminal temperatures agree with predictions. The heat exchanger performance assessment is incomplete; more study is required to quantify the heat exchanger effectiveness.

In addition, better CM and cavity construction techniques and procedures have incrementally improved the thermal performance.

6.4 The CEBAF C100 Energy Upgrade Cryomodule

6.4.1 Introduction

In 2008 construction began on the energy upgrade of the CEBAF accelerator to 12 GeV [20]. To achieve the 12 GeV energy five new cryomodules were added to each of the two existing linacs. Each cryomodule provides 100 MV of accelerating voltage with eight 1500 MHz SRF cavities. Each cavity contains seven 1500 MHz cells, two hook style HOM couplers, and a FPC [21]. Each cavity has 0.7 m of active length and is required to operate at 19.2 MV/m to provide the 100 MV of required voltage and have sufficient voltage overhead for robust operations. A new low loss cell geometry [22] is used to reduce the 2 K heat load. The cavities, cryomodule, and helium refrigerator are designed for a total of 300 W 2 K heat load for each cryomodule. The cavity and cryomodule alignment requirements remain unchanged from the original CEBAF specification [23]. The C100 cryomodules (see Fig. 6.21) are installed in existing empty linac zones and are required to maintain the same cryogenic circuits and interfaces as the C20 cryomodules (see Fig. 6.22).

6.4.2 Lessons Learned from C20 Experience

The C100 cryomodule design benefited from the production and decade of operations of the C20 cryomodules as well as advances in the SRF technology and

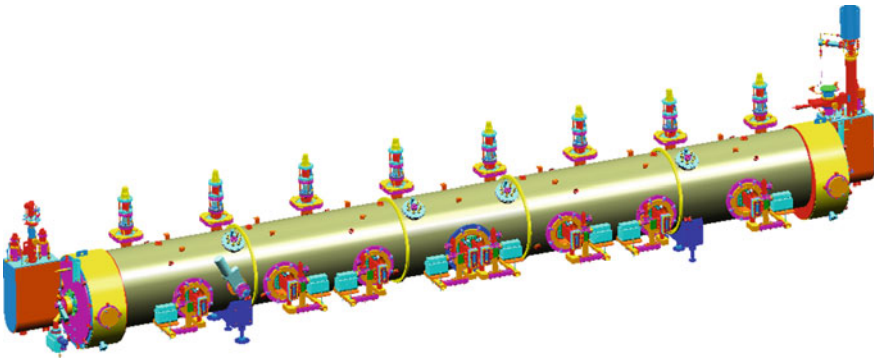

Fig. 6.21 C100 cryomodule assembly

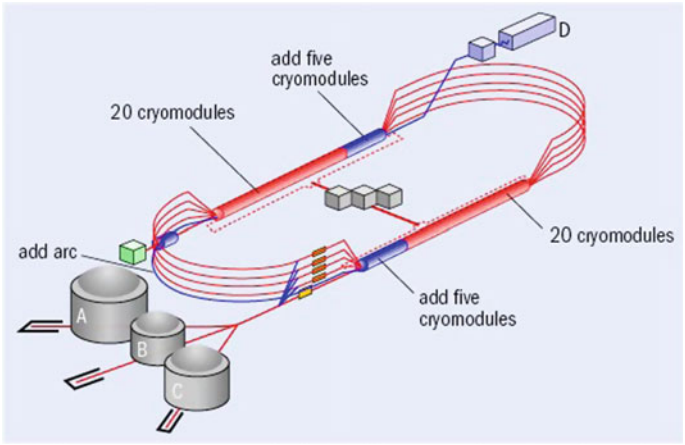

Fig. 6.22 12 GeV CEBAF with ten C100 cryomodules

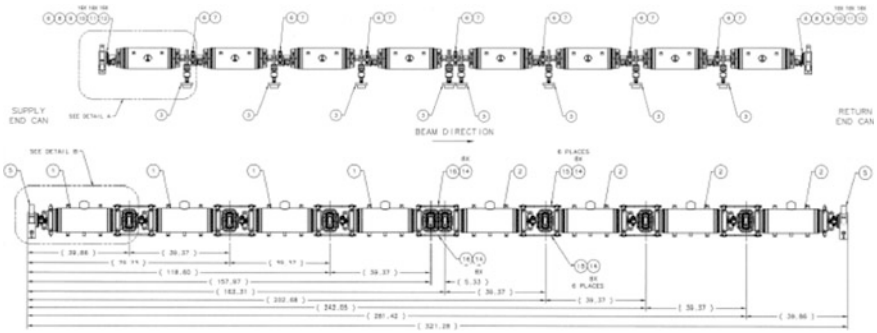

Fig. 6.23 C100 cavity string

facilities. The largest change in the C100 cryomodule was the move away from a cavity pair assembly used as the basis for the C20 cryomodule to an eight cavity string (see Fig. 6.23) assembled in the clean room. The cavity string assembly is too large to be tested prior to assembly into a cryomodule. This requires each cavity to be vented after being tested individually prior to being assembled into the cavity string. This use of a cavity string assembly is based on a high level of confidence that the cavity performance will be maintained after the string assembly process. This confidence comes from the cavity design that eliminates all indium seals, improved cleaning techniques including high pressure water rinsing, improved cleanrooms, assembly tooling, and procedures as well as demonstrated performance.

Another significant change to the design was moving all the cavity frequency tuner friction bearing components outside the helium and vacuum space. This eliminates motors and gears operating at cryogenic temperatures and in a vacuum. Important features retained from the C20 cryomodule include using all welded

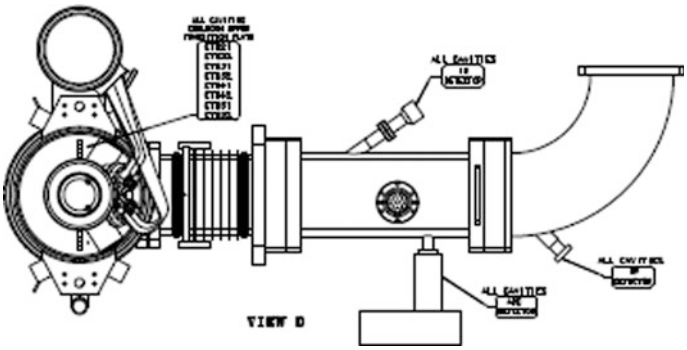

Fig. 6.24 C100 FPC assembly with the cavity and helium circuits

stainless steel cryogenic circuits including the helium vessel, a double RF window FPC, and individual heaters for each cavity that are inside the helium vessels. The stainless steel cryogenic circuit construction provides a high reliability fabrication avoiding leaks from flanged connections at a minimum cost. Some instrumentation flanges are required to route temperature, level, and heater signals out of the cryogenic circuits. These are kept to a minimum and are done with smaller knife edge seal flanges that undergo rigorous QC checks including cold shocking and leak checking prior to use. The double RF window on the FPC provides redundancy against vacuum leaks that can be a problem on high power RF transmission lines. The space between the two windows creates an intermediate vacuum space that can be monitored for off normal conditions and shutdown RF to avoid catastrophic failures (see Fig. 6.24).

The individual heaters are important for balancing the dissipated power on a cavity by cavity basis on a high power cryomodule and provide for high resolution cavity performance measurements [24] when used in a segmented cryomodule with isolation valves like the CEBAF cryomodules.

6.4.3 Cavity

The SRF cavity is a 1500 MHz seven cell cavity with a close fitting, 10 in. OD, stainless steel helium vessel (see Fig. 6.25). The transition from the Niobium cavity to the stainless steel is done with a brazed assembly incorporated into the beamline just outside of the cavities [25]. The FPC, HOM couplers, and RF pickup probe are located outside of the helium vessel. The cavity assembly includes flanged interfaces for each of these and the two beamline connections. Unlike the original CEBAF cavity where the FPC and HOM and RF pickup probes are located inside the helium vessel, on the C100 cavity these elements are located in the insulating

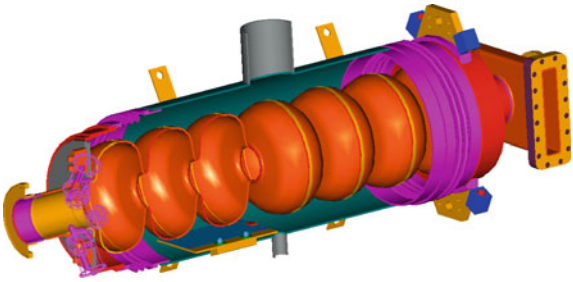

Fig. 6.25 C100 cavity cut assembly with helium vessel

vacuum space. This requires careful attention to the thermal management [26] as all heat must be conductively removed to the helium inside the helium vessel. The resulting temperature gradient can increase the beamline temperature enough to make them normal conducting. Most often this results in a thermal quench of the cavity. Early on this was a limit in the C100 cavities. The niobium HOM pickup probes would heat from the fundamental mode RF currents and above a certain operating gradient would transition to the normal conducting state and quench the cavity. JLab developed very high thermal conducting RF feedthroughs [27] to shunt the heat from the HOM pickup probe away from the cavity.

6.4.4 Cavity Frequency Tuner

The cavity frequency tuner design (see Fig. 6.26) was a radical change from the existing CEBAF tuner [28]. Based on lessons learned from the C20 experience all friction bearing components were placed outside the insulating vacuum space and can be replaced with the cryomodule cold. The tuner actuator has a stepper motor coupled to a harmonic drive reducer for coarse tuning and a piezo actuator for fine tuning. The tuner has a minimum range of 400 kHz and a resolution of 1 Hz. The tuning motion of the drive system enters the cryostat through two thin-wall concentric tubes. The tubes are connected to the upper and lower arms of a scissors type jack. The axial motion of the tubes translates into a linear stroke parallel to the cavity center line. To eliminate friction, motion within the vacuum is done with flexure plates.

6.4.5 Cold Mass and Space frame

The C100 cryomodule uses a cold mass subassembly made up of the cavity string (Fig. 6.27), cold magnetic shielding, cavity frequency tuners, cryogenic piping, and associated instrumentation [29]. The cold mass assembly length is constrained to fit into the existing slot length of the original cryomodule while increasing the active

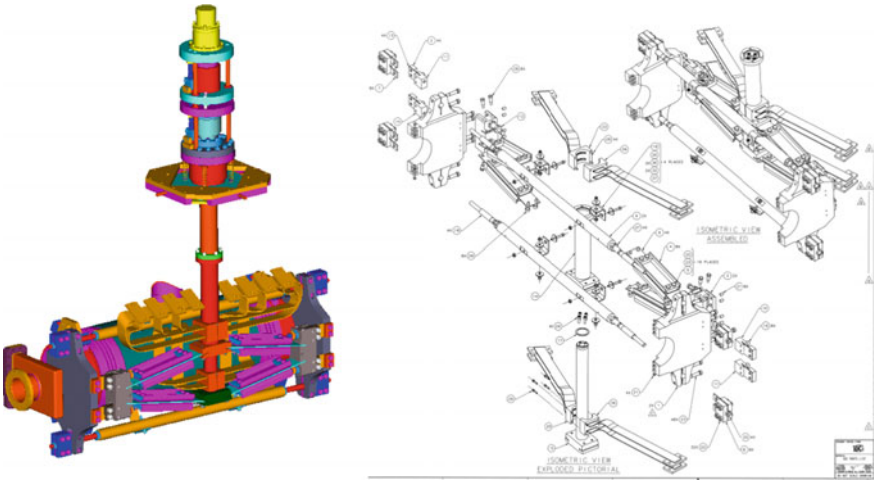

Fig. 6.26 C100 tuner

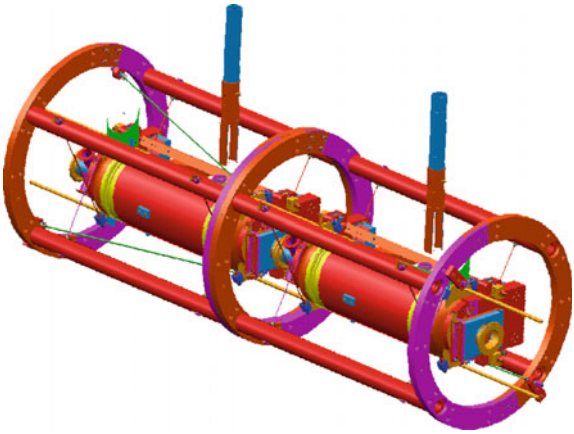

Fig. 6.27 Cavity string anchoring at the center of the space frame using nitronic rods

cavity length by 40 %. The increased cavity length is accommodated by the elimination of all bellows between the cavities. The cavity string is anchored in the center of the cryomodule and all cooldown and cavity tuning effects must be managed over the entire length of the four cavity half string extending out from the center to the end of the cryomodule.

There are vacuum boundaries that extend from the cold mass to the warm vacuum vessel at each cavity for the FPC and one at each end of the cavity string (see Fig. 6.28). The relative movement at the cavity string ends is provided for by the use of two multi-convulsion stainless steel bellows in series integrated into the warm to cold beamline transition. There is a shield intercept point between the two bellows minimizing the heat load to the shield and primary cryogenic circuit.

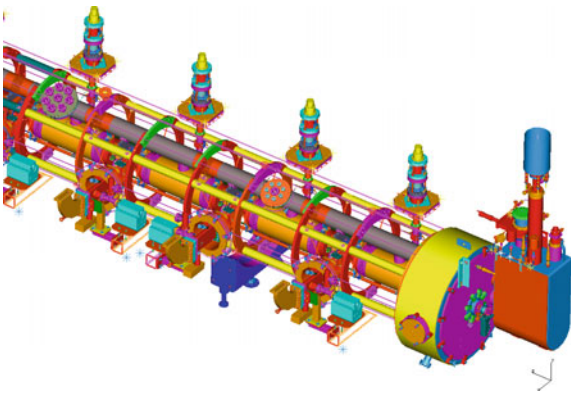

Fig. 6.28 Cryomodule cut away showing the cold mass and space frame

The FPC is rectangular section mounted normal to the direction of movement which has two 3 convulsion bellows along its length separated as much as possible resulting in a dogleg motion producing the required relative movement between the cavity and vacuum vessel.

The cold mass is supported by the space frame (see Fig. 6.27). The space frame provides advantages over supporting from the vacuum vessel [30]. The first is that it allows all the assembly to take place outside the vacuum vessel (where things are more readily accessible). The space frame with all the cryounits attached, is then rolled into the vacuum vessel and locked down. The second advantage is the requirement for fewer penetrations in the vacuum vessel, thus reducing cost and possibility of vacuum leaks.

The space frame also supplies points for aligning the beam line while inside the vacuum vessel. The space frame consists of a series of five welded tube and ring sections of 304 stainless steel bolted together. The tubes are 2.5 in. outer diameter with a 0.25 in. wall thickness. The rings are 29.75 in. outer diameter, 23.75 inner diameter by 0.75 in. thick. The tubes are fitted to the rings in a socket joint and welded.

The cavities are suspended from the space frame support tubes using nitronic rods. There are eight 0.198 in. diameter rods connected to each unit. The rods have a silicon bronze swaged, threaded fitting attached to each end. The rods are extended to the opposite side of the He vessel in order to increase the length and keep the static heat load to a minimum.

All the mass of the space frame and attachments is supported by 4 stainless steel wheels at the "quarter" points of the frame. Any axial loading (2 g transport loads) is supported by two brackets at one of the quarter points.

6.4.6 Vacuum Vessel

The vacuum vessel defines the air to insulating vacuum interface. The space frame with the cold mass is inserted axially into the vessel. End caps and tophats are

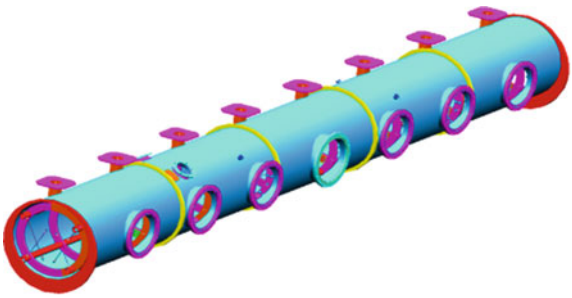

Fig. 6.29 Vacuum vessel

installed to complete the cryomodule. The vacuum Vessel consists of 0.25 in. thick 304 stainless steel rolled to a 32 in. outer diameter cylinder. Five sections approximately 61 in. long are welded together using a support ring at each joint and the ends. The support ring is 1 in. thick with a 35 in. outer diameter. There are six 15.5 in. openings and one 17.5 in. opening for waveguide attachment. Also, there are eight 4.5 in. openings for the tuners. Various other small openings for alignment and lockdown access are also included (Fig. 6.29). The vacuum vessel is supported by two saddle stands, one at each "quarter point". The space frame (wheels) is supported by the vacuum vessel at the same points, thus only adding compression stresses into local areas of the wall under normal loading. The space frame is also locked down axially to the vessel via a plate protruding from the space frame, which is trapped in a bracket and welded to the vacuum vessel. There is a spring relief plate located at both ends to limit the internal pressure to less than 2 atm.

6.4.7 End Cans

The End cans for the C100 cryomodule are adapted from the original CEBAF C20 end cans. The primary and shield circuits are connected to the distribution system using removable u-tubes with bayonet connections. Each end can bayonet has an isolation valve allowing u-tubes to be removed and installed while the cryomodule and distribution system are cold. Every volume that can be isolated with valves includes a relief valve to avoid over pressurization in case cold gas is allowed to warm in the potential trapped volume. The supply and return end can piping consists of the primary circuit, which provides cooling fluid to the superconducting cavities, and the shield circuit that cools the nominal 50 K thermal shield. The gas/fluid circuits consist of pipes, tubes, fittings, and valves. The design pressure for the primary circuit is 5.0 and 20.0 atm for the shield circuit [31]. The end plate has a pass through for the beampipe with an O-ring sealing surface as well as a shield thermal strap to minimize the conduction heat load to the 2 K circuit.

6.4.8 C100 Performance

Ten C100 cryomodules have been installed and operated in the CEBAF accelerator. Early commissioning of the first cryomodules included high current operations at 108 MV accelerating voltage meeting the design goals. Commissioning results show that these cryomodules will deliver an average energy gain of 110 meV which exceeds the design goal of 108 MV. The C100 cavities are able to operate at an average maximum operating gradient of 19.6 MV/m [32]. Early operations identified challenges to stable operations due to microphonics. As a result the tuner end plates were made stiffer significantly reducing the transmission of vibrations to the cavities.

6.5 SSR1 Cryomodule Design for PXIE

6.5.1 Introduction

Fermilab is in the process of designing a Project X Injector Experiment (PXIE), a CW linac, to validate the Project X concept, reduce technical risks, and obtain experience in the design and operation of a superconducting proton linac. The overall facility will include an ion source, low and medium-energy beam transport sections, an RF quadrupole, and two superconducting cavity cryomodules. One will contain eight half-wave resonators operating at 162.5 MHz and eight superconducting solenoids. The second will contain eight single spoke resonators (SSR1) operating at 325 MHz and four superconducting solenoids. The design of the cryomodule being developed to house the 325 MHz single spoke resonators and all related systems and services is described here.

The SSR1 cryomodule will operate with continuous wave (CW) RF power and support peak currents of 5 mA chopped with arbitrary patterns to yield an average beam current of 1 mA. The RF coupler design employed should support a future upgrade path with average currents as high as 5 mA. The RF power per cavity at 1 mA average current and 2.2 MV accelerating voltage ($\beta = 0.22$) should not exceed 4 KW with an overhead reserved for microphonics control. The RMS normalized bunch emittance at the CM exit should not exceed 0.25 mm mrad for each of 3 planes.

The current beam optics design for Project X requires that the SSR1 cryomodule contains eight cavities (C) and four solenoids (S) in the following order: C–S–C–C–S–C–C–S–C–C–S–C. Horizontal and vertical dipole corrector are located inside each solenoid. A four-electrode beam position monitor is located at each solenoid.

The intent is that this cryomodule will have all external connections to the cryogenic, RF, and instrumentation systems made at removable junctions at the cryomodule itself. The only connection to the beamline is the beam pipe itself which will be terminated by “particle free” valves at both ends. Minimizing mean

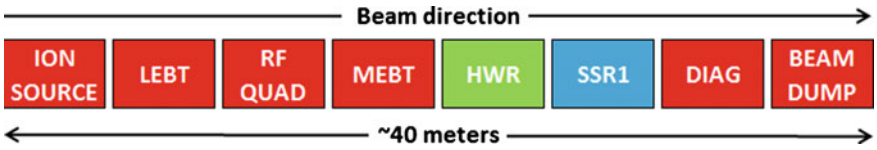

Fig. 6.30 PXIE layout

time between failure and repair and in situ repair of some internal systems are important design considerations in the cryomodule design. Figure 6.30 shows the linac layout including the location of the SSR1 cryomodule. Table 6.7 lists pertinent operational requirements and parameters of the cryomodule assembly.

6.5.2 Cryomodule Design

Eventually, Project X will require several different cryomodule designs for cavities operating at 162.5, 325, 650, and 1300 MHz. The SSR1 for PXIE is the first of these being developed at Fermilab. Some details of individual cryomodule components are described in the following sections.

6.5.2.1 Cryogenic Systems and Vacuum Interfaces

Fine segmentation is the configuration choice for Project X and PXIE cryomodules. Each individual vacuum vessel will be closed at both ends and the cryogenic circuits will be fed through bayonet connections at each cryomodule. Each cryomodule will have its own connection to the insulating vacuum pumping system. Also, each cryomodule will have its own 2 K heat exchanger and pressure relief line exiting near the middle of the module. This configuration provides flexibility in terms of cryomodule replacement, and cooldown and warm-up times at the expense of requiring more individual cryogenic connections, cold-to-warm transitions at each end of each cryomodule, and extra space at each interconnect to close the beam tube.

6.5.2.2 Vacuum Vessel

The vacuum vessel serves to house all the cryomodule components in their as-installed positions, to provide a secure anchor to the tunnel floor, to insulate all cryogenic components in order to minimize heat load to 80, 4.5, and 2 K, as well as maintain the insulating vacuum. It is 1.219 m (48 in.) in diameter and manufactured from carbon steel and is shown as the outermost shell in Fig. 6.37.

Table 6.7 SSR1 functional requirements specifications (subject to change)

General	
Physical beam aperture, mm	30
Overall length (flange-to-flange), m	≤5.4
Overall width, m	≤1.6
Beamline height from the floor, m	1.3
Cryomodule height (from floor), m	≤2.00
Ceiling height in the tunnel, m	3.20
Maximum allowed heat load to 70 K, W	250
Maximum allowed heat load to 5 K, W	80
Maximum allowed heat load to 2 K, W	50
Maximum number of lifetime thermal cycles	50
Intermediate thermal shield temperature, K	45–80
Thermal intercept temperatures, K	5 and 45–80
Cryo-system pressure stability at 2 K (RMS), mbar	~0.1
Environmental contribution to internal field	15 mG
Transverse cavity alignment error, mm RMS	<1
Angular cavity alignment error, mrad RMS	≤10
Transverse solenoid alignment error, mm RMS	<0.5
Angular solenoid alignment error, mrad RMS	<1
Cavities	
Number, total	8
Frequency, MHz	325
β geometric	0.22
Operating temperature, K	2
Operating mode	CW
Operating energy gain at β = 0.22, MV/cavity	2
Coupler type—standard coaxial with impedance, Ω	105
Coupler power rating, KW	>20
Solenoids	
Number, total	4
Operating temperature, K	2
Current at maximum strength, A	≤100
$\int B^2 dL$, T^2m	4.0
Each solenoid has independent powering	
Correctors	
Number, total	8
Number, per solenoid package	2
Current, A	≤50
Strength, T-m	0.0025
Beam position monitors	
Number, total	4
Number of plates	4
Electrical center accuracy compared to geometric center, mm	≤±0.5

6.5.2.3 Magnetic Shield

Just inside the vacuum vessel, virtually in contact with the inner wall, is a magnetic shield to shield the cavities from the earth's magnetic field. Preliminary tests show that a 1.5 mm-thick mu-metal shield at room temperature reduces the residual field inside the cryostat to less than 10 μT. It is likely that separate magnetic shields will be installed around individual magnetic elements to further reduce the potential for trapped fields in the superconducting cavity structures.

6.5.2.4 Thermal Shield and Multilayer Insulation

Each cryomodule will have a single thermal shield cooled with helium gas, nominally at 45–80 K. It is currently envisioned to be made from 6000-series aluminum with cooling channels on both sides. Two 15-layer blankets of multilayer insulation, between the vacuum vessel and thermal shield will reduce the radiation heat load from the room temperature vacuum vessel to approximately 1.5 W/m2. A 5 K circuit will be available to intercept heat on the input couplers and current leads, but there is no plan to install a full 5 K thermal shield.

6.5.2.5 Support System

All of the cavities and solenoids will be mounted on individual support posts which are in turn mounted to a full-length strongback located between the vacuum vessel and thermal shield. This enables the entire cavity string to be assembled and aligned as a unit then inserted into the vacuum vessel during final assembly. The strongback is aluminum to provide a uniform temperature base. Maintaining the strongback at room temperature helps minimize axial movement of the cold elements during cooldown, reducing displacement of couplers, current leads, and many of the internal piping components.

The support posts are similar to supports utilized in SSC collider dipole magnets (Chap. 2) and ILC and XFEL 1.3 GHz cavity cryomodules (Chap. 5). The main structural element is a glass and epoxy composite tube. The tube ends and any intermediate thermal intercepts are all assembled using conventional shrink-fit assembly techniques in which the composite tube is sandwiched between an outer metal ring and inner metal disk. The strongback and support posts are shown in Fig. 6.31. All of the cavities and magnetic elements are mounted to the support posts using adjustable positioning mechanisms [33].

6.5.2.6 Cavity and Tuner

The cryomodule contains eight single spoke, $\beta = 0.22$, 325 MHz cavities operating in CW mode at 2 K in stainless steel helium vessels. Each has an integral coarse

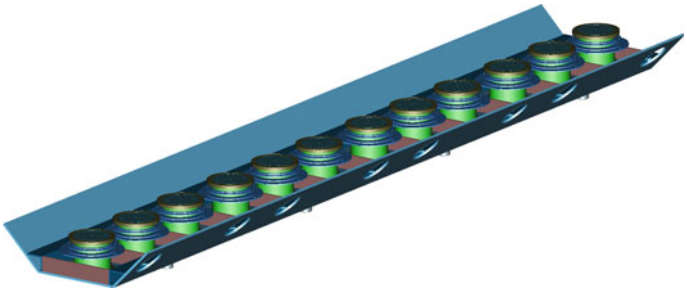

Fig. 6.31 Strongback with supports

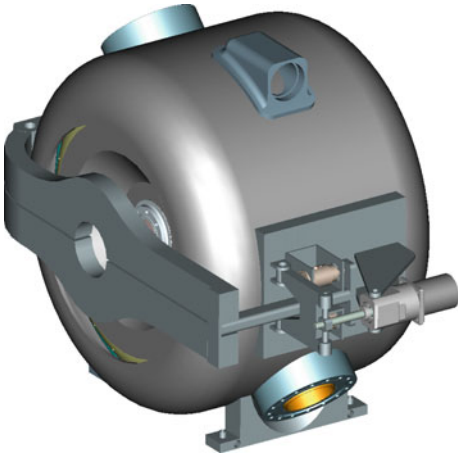

Fig. 6.32 Spoke cavity, helium vessel, and tuner

and fine tuner that operates through a lever system and pushes on the cavity end wall. For ease of maintenance, tuner access covers are incorporated into the helium vessel design. The cavity and tuner system is shown in Fig. 6.32 and described more completely in [34].

6.5.2.7 Input Coupler

The input coupler is a 105-ohm coaxial design that supplies approximately 2 kW CW to each cavity in PXIE and ultimately up to 18 kW CW in Project X. The coupler contains a single warm ceramic window that provides separation of the warm and cold coupler sections. During cryomodule fabrication, the cold section can be installed on the cavity in the cleanroom prior to assembly of the string. The warm section can then be installed from outside the vacuum vessel during final assembly. The inner conductor is solid copper with copper bellows to accommodate motion due to misalignment and thermal contraction. The cold end of the outer conductor is 316L-stainless steel. The warm end is copper with copper bellows.

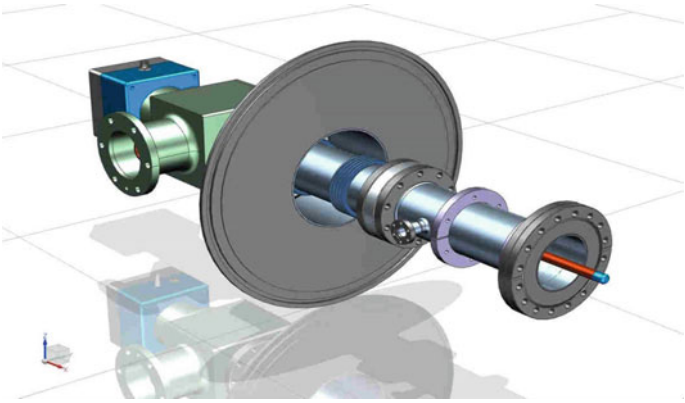

Fig. 6.33 Input coupler

Heat load estimates don't suggest a significant penalty for not copper plating the outer conductor. A forced-air cooling tube is inserted into the inner conductor after assembly that supplies air to cool the coupler tip. Figure 6.33 shows the current coupler design. The input coupler design is described more thoroughly in [35].

6.5.2.8 Current Leads

Each focusing element package contains up to three magnet coils, the main solenoid, operating nominally at 100 A and two steering correctors each operating nominally at 50 A. A conduction cooled current lead design modeled after similar leads installed in the LHC at CERN is being developed for use in the SSR1 cryomodule [36]. Figure 6.34 illustrates the design for the lead assembly. Thermal intercepts at 45–80 K and at 5 K help reduce the heat load to 2 K, nonetheless, these current leads represent a significant source of heat at the low temperature end. There will be one lead assembly for each magnetic element.

6.5.2.9 Solenoid and Beam Position Monitor

The four magnet packages in the cryomodule each contain a focusing solenoid and two dipole correctors all operating in a helium bath at 2 K. The Project X lattice, especially the low-beta section, provides little room along the beamline for beam diagnostics either inside individual cryomodules or between adjacent modules. In order to conserve axial space along the beamline a button-type beam position monitor (BPM) was chosen for installation in the SSR cryomodules. A total of four will be installed in the cryomodule and tested in PXIE, one at each magnetic element. These devices are compact and lend themselves well to incorporation right into the solenoid magnet package as shown below in Fig. 6.35. The bellows in either end of the beam tube allow independent adjustment of each magnet.

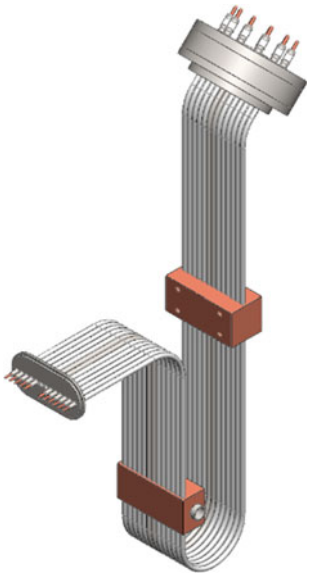

Fig. 6.34 Conduction cooled current lead assembly

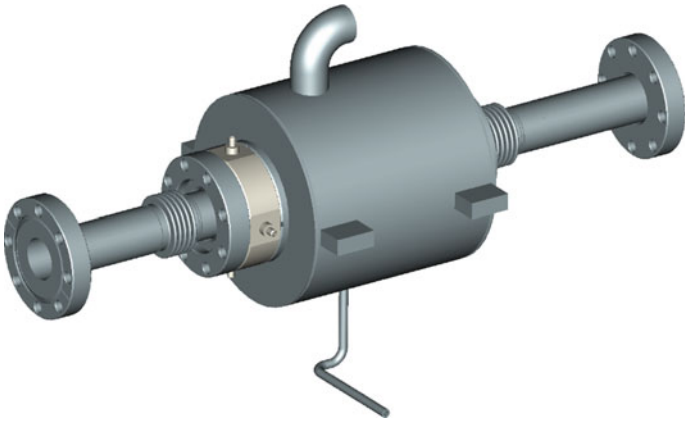

Fig. 6.35 Solenoid and BPM assembly

6.5.3 Final Assembly

The final assembly of the SSR1 cryomodule for PXIE is shown in Figs. 6.36 and 6.37. Figure 6.36 shows the cavity string consisting of the cavities, solenoids, beam position monitors, and internal piping mounted on support posts which are in turn mounted to the strongback. Figure 6.37 shows the entire cryomodule assembly.

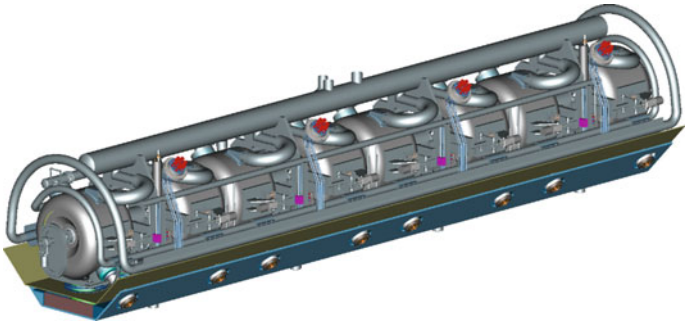

Fig. 6.36 Cavity string assembly

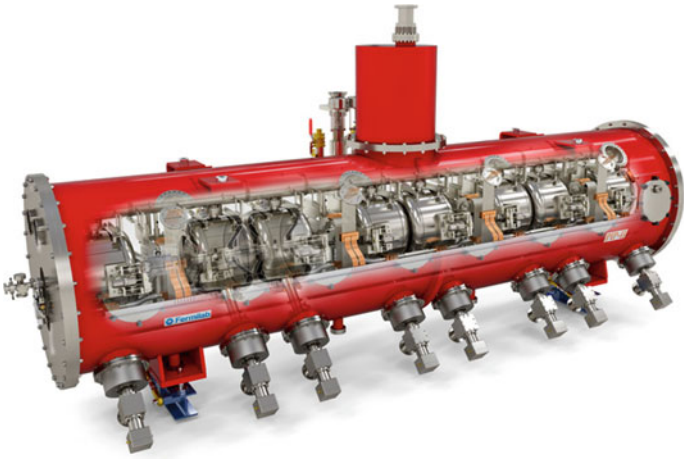

Fig. 6.37 Cryomodule assembly

6.5.4 Status and Plans

Fermilab has the PXIE SSR1 vacuum vessel, cavities, strongback, support posts, and many other cryomodule components in-house. Work is in the process to build up production facilities, develop assembly procedures for the cavity string, and to tooling for insertion of the cavity string into the cryomodule. Installation of the cryomodule in the PXIE facility is expected in 2017 [37].

References

1. G. Oliver, J.P. Thermeau, P. Bosland, G. Devanz, F. Lesigneur, C. Darve, *ESS Cryomodule for Elliptical Cavities*, Proceedings of the 16th International Conference on RF Superconductivity (2013)
2. M. Johnson et al., *Design of the FRIB Cryomodule*, IPAC 2012, New Orleans (2012)
3. H.A. Grunder et al., in *The Continuous Electron Beam Accelerator Facility*, ed. by E.R. Lindsrom, L.S. Taylor. Proceedings of the 1987 IEEE Particle Accelerator Conference, vol. 1 (Washington, D.C., 1987), pp. 13–18
4. C. Reece et al., in *Production Vertical Cavity Pair Testing at CEBAF*, Proceedings of the Particle Accelerator Conference (1993), pp. 650–658
5. C.H. Rode et al., 2.0 K CEBAF CRYOGENICS, CEBAF PR-89-029
6. D. Kashy et al., CEBAF transfer line system, CEBAF PR-91-024 June 1991
7. M. Wiseman et al., CEBAF cryounit loss of vacuum experiment. Appl. Cryog. Technol. **10**, 287–303
8. W. Schneider et al., Thermal performance of the CEBAF superconducting linac cryomodule. Adv. Cryog. Eng. **39**, 589–596
9. J. Benesch et al., CEBAF's SRF cavity manufacturing experience. Adv. Cryog. Eng. **39**, 597–604
10. M. Wiseman, et al, Cryobench—Apparatus for testing cryogenic subcomponents, Appl. Cryog. Technol. **10**, 271–285
11. J.P. Kelley et al., Thermal design and evaluation of the CEBAF superconducting RF cavity's prototype waveguide. Adv. Cryog. Eng. **35**, 675–682 (1990)
12. I.E. Campisi et al., Higher-order-mode damping and microwave absorption at 2 K, EPAC 92, vol. 2
13. G. Ciovati et al., Superconducting prototype cavities for the spallation neutron source (SNS) project. PAC2001, Chicago, IL, June 2001
14. I.E. Campisi et al., The fundamental power coupler for the spallation neutron source (SNS) project. PAC2001, Chicago, IL, June 2001
15. T. Whitlatch et al., Shipping and alignment for the SNS cryomodule. PAC2001, Chicago, IL, June 2001
16. J. Hogan et al., Design of the SNS Cavity Support Structure, PAC2001, Chicago, IL, June 2001
17. T. Whitlatch et al., Shipping and alignment for the SNS Cryomodule. PAC2001, Chicago, IL, June 2001
18. W. Schneider et al., *Thermal Performance of the CEBAF Superconducting Linac Cryomodule*. Advances in Cryogenic Engineering, vol. 39 (Plenum Press, New York, 1994), pp. 589–597
19. D. Kashy et al., CEBAF *Transfer Line Systems*. Advances in Cryogenic Engineering, vol. 37 (Plenum Press, New York, 1992), pp. 577–586
20. L. Cardman, L. Harwood, in *The JLab 12 GeV Energy Upgrade of CEBAF for QCD and Hadronic Physics*, Proceedings of PAC07, pp. 58–62
21. C.E. Reece et al., in *Optimization of the SRF cavity Design for the CEBAF 12 GeV Upgrade*, Proceeding of the 13th International Workshop on RF Superconductivity
22. J. Sekutowicz et al., in *Cavities for JLab's 12 GeV Upgrade*, Proccedings of the 2003 Particle Accelerator Conference
23. D. Douglas, J. Preble, JLAB-TN-98-022
24. M. Drury et al., *Commissioning of the CEBAF Cryomodules*, Proceedings of the 1993 Particle Accelerator Conference, pp. 841–843
25. R. Hicks, JLAB-TN-07-037
26. R. Hicks, E. Daly, JLAB-TN-02-040, *Thermal Analysis of a 13 kW Waveguide for the 12 GeV Upgrade Cryomodule*
27. C. Reece et al., *High Thermal Conductivity Cryogenic RF Feedthroughs for Higher Order Mode Couplers*, Proceedings of 2005 Particle Accelerator Conference

28. K. Davis et al., *Development and Testing of a Prototype Tuner for The CEBAF Upgrade Cryomodule*, Proceedings of the 2001 Particle Accelerator Conference, pp. 1149–1151
29. J. Hogan et al., Design of the CEBAF Energy Upgrade Cryomodule Cold Mass. Proceedings of the 2001 Particle Accelerator Conference, pp. 1595–1597
30. T. Whitlatch, Space frame structural analysis for the CEBAF upgrade cryomodule, JLAB-TN-00-002
31. G. Chang, E. Daly, C100 cryomodule end can piping design pe ASME B31.3, JLAB-TN-07-056
32. M. Drury et al., *CEBAF upgrade: cryomodule performance and lessons learned*, Proceedings of SRF2013, pp. 836–843
33. T.H. Nicol, R.C. Niemann, J.D. Gonczy, *Design and Analysis of the SSC Dipole Magnet Suspension System*, Supercollider 1 (Plenum Press, New York, 1989), pp. 637–649
34. L. Ristori, et al., Design of single spoke resonators for PXIE. Presented at IPAC 2012, paper ID: 2689-WEPPC057
35. S. Kazakov, et al., Main couplers design for project X. Presented at IPAC 2012, paper ID: 2523-WEPPC050
36. A. Ballarino, Conduction-cooled 60 a resistive current leads for LHC dipole correctors, LHC Project Report 691, 2004
37. T.H. Nicol, G. Lanfranco, L. Ristori, High intensity neutrino source superconducting spoke resonator and test cryostat design and status. IEEE Trans. Appl. Supercond. **19**(3), 1432–1435 (2009)